DEFENCE R&D DÉFENSE

Chaotic Sea Clutter Returns

Current Status and Application to Airborne Radar Systems

Michael K. McDonald

Defence R&D Canada
TECHNICAL REPORT
DREO TR 2001-114
November 2001

National Defence Défense nationale

Canada

Chaotic Sea Clutter Returns

Current Status and Application to Airborne Radar Systems

Michael K. McDonald
Surveillance Radar Group
Aerospace Radar and Navigation Section

DEFENCE RESEARCH ESTABLISHMENT OTTAWA

TECHNICAL REPORT

DREO TR 2001-114

NOVEMBER 2001

Abstract

The potential to model sea clutter radar returns using chaos theory is examined. Chaotic systems display qualitative similarities to sea clutter returns such as broad flat spectrums, boundedness and irregular temporal behaviour. In this report several key parameters of chaotic systems, namely correlation dimension, Lyapunov spectrum and Lyapunov dimension are calculated from real sea clutter returns and found to be consistent with a chaotic interpretation. The airborne high resolution data (less than one metre) produces a correlation coefficient with an average value of 4.63 and an embedding dimension of 6-7. Lyapunov dimensions are consistent with correlation values. A local linear technique and a radial basis function (RBF) are used to construct a one step non-linear predictor. A Mean Square Error (MSE) of approximately 0.0032 between the predicted and normalized (i.e. maximum +/- 1 range) real time series is measured. If sea clutter is in fact, a chaotic system, then it may be possible to accurately predict sea clutter returns via a non-linear chaotic model and produce substantial improvements in the small target detection capabilities of the APS-506 radar on the CP-140 maritime patrol aircraft.

Résumé

On étudie la possibilité de modéliser le clutter radar de mer à l'aide de la théorie du chaos. Les sytèmes chaotiques présentent des similitudes qualitatives avec le clutter de mer, par exemple de larges spectres plats, la limitabilité et un comportement temporel irrégulier. Dans le présent rapport, plusieurs paramètres clés des systèmes chaotiques, notamment la dimension de corrélation, le spectre de Lyapunov et la dimension de Lyapunov, sont calculés à partir d'un clutter de mer réel, et on constate qu'ils sont compatibles avec une interprétation basée sur la théorie du chaos. Avec les données aériennes à haute résolution (moins de un mètre), on obtient un coefficient de corrélation moyen de 4,63 et une dimension de prolongement de 6-7. Les dimensions de Lyapunov sont compatibles avec les valeurs de corrélation. Une technique linéraire locale et une fonction de base radiale (FBR) sont utilisées pour établir un prédicteur non linéaire à une étape. Une erreur quadratique moyenne (EQM) égale approximativement à 0,0032 entre les séries chronologiques prévues et les séries réelles normalisées est obtenue.

This page intentionally left blank.

Executive summary

The study of radar detection of small targets in clutter has traditionally relied on the application of stochastic theory to the development of target detection schemes. In theory, modelling sea clutter with an appropriate statistical distribution allows the calculation of the detection probability for a specified false alarm rate. This approach assumes that clutter returns are stochastic processes with infinite degrees of freedom, or at the very least, processes that have such a large number of degrees of freedom that the only practical approach is to model them as stochastic processes. Qualitatively a stochastic interpretation appears to be consistent with real clutter return spectrums, which are typically highly irregular in character and have continuous broadband spectrums reminiscent of broadband noise.

In contrast to stochastic methods it has recently been suggested that sea clutter returns can be modelled using chaos theory. Chaotic systems are non-linear dynamic systems with a relatively small number of degrees of freedoms. These deterministic dynamic systems have the unusual property of displaying irregular behaviour and broad flat spectrums. If it can be shown that sea clutter is in fact, a chaotic system, and the function describing it can somehow be determined, then the deterministic nature of a chaotic solution should prove more informative. The ultimate goal of applying chaotic theory to the sea clutter problem is to exploit its deterministic nature so as to develop accurate predictors for sea clutter returns. This ability to accurately predict sea clutter returns via a non-linear chaotic model should, in theory, produce substantial improvements in detection performance over that of stochastic models and in particular, improve the small target detection capabilities of the APS-506 radar on the CP-140 maritime patrol aircraft.

This report examines the behaviour and characteristics of chaotic systems. Past attempts to identify chaotic behaviour in radar returns from sea clutter are reviewed and summarized. Most of the past work has focussed on the studies of returns from relatively low resolution radars (i.e. range resolutions of greater than 30 metres) operating in a staring mode from a land based position overlooking the sea. This study extends the previous work which showed that the calculated correlation coefficients of real sea clutter were independent of the time or season in which it is taken, as well as radar range, range resolution, type of like-polarisation, sea state, radar location and radar type. In this report high resolution data (less than one metre) collected using the AN/APS-506 airborne maritime surveillance are analysed. Several key parameters of chaotic systems, namely correlation dimension, Lyapunov spectrum and Lyapunov dimension are calculated from the real sea clutter returns and found to be consistent with a chaotic interpretation.

The deterministic character of the sea clutter returns is tested by developing a one step non-linear predictor. Two different approaches are implemented, a local linear technique and a radial basis function (RBF) neural network. Good performance is achieved with a mean square error (MSE) of approximately 0.0032 measured between the predicted and real time series, both of which have been normalized to have a maximum range of +/- 1.

McDonald, Michael K. 2001. Chaotic Sea Clutter Returns: Current Status and Application to Airborne Radar Systems. DREO TR 2001-114 Defence Research EstablishmentOttawa.

Sommaire

L'étude de la détection radar en présence de clutter a par le passé reposé sur l'application de la théorie stochastique pour l'élaboration de plans de détection de cible. En théorie, la modélisation du clutter de mer au moyen d'une distribution statistique appropriée permet de calculer la probabilité de détection pour un taux de fausse alarme constant donné. Dans cette approche, on considère que le clutter est un processus stochastique avec un nombre infini de degrés de liberté, ou tout au moins un processus comportant un nombre tellement élevé de degrés de liberté que la seule méthode pratique applicable pour le modéliser consiste à le considérer comme un processus stochastique. Qualitativement, une interprétation stochastique semble être compatible avec les spectres observés de clutter réel, lequel est habituellement de nature très irrégulière et présente des spectres continus à large bande qui rappellent un bruit à large bande.

Bien qu'une grande importance soit accordée aux méthodes stochastiques, on a récemment suggéré que le clutter de mer pourrait être modélisé à l'aide de la théorie du chaos. Les systèmes chaotiques sont des systèmes dynamiques non linéaires possédant un nombre relativement faible de degrés de liberté. Ces systèmes déterministes dynamiques ont la propriété peu courante de présenter un comportement irrégulier et de larges spectres plats. Si on peut démontrer que le clutter de mer est en réalité un système chaotique, et que la fonction servant à le décrire peut d'une façon ou d'une autre être déterminée, la nature déterministe d'une solution chaotique devrait se révéler plus riche en information que la solution stochastique, ce qui devrait se traduire par une modélisation et des capacités de détection améliorées.

Dans le présent rapport, on étudie le comportement et les caractéristiques de systèmes chaotiques. Les tentatives antérieures visant à détecter le comportement chaotique du clutter radar de mer sont examinées et résumées. La plupart des travaux antérieurs étaient axés sur les études des échos obtenus avec des radars à résolution relativement faible (résolutions en distance supérieures à 30 mètres) utilisés en mode sans balayage à partir d'une position au sol donnant sur la mer. L'étude approfondit les travaux antérieurs, lesquels ont montré que les coefficients de corrélation calculés du clutter de mer réel étaient indépendants de l'heure ou de la saison à laquelle ils étaient déterminés, ainsi que de la portée radar, de la résolution en distance, du type de polarisation parallèle, de l'état de la mer, et de la position et du type du radar. Dans le présent rapport, des données à haute résolution (moins de un mètre) recueillies à l'aide du radar aérien de surveillance maritime AN/APS-506 sont analysées. Plusieurs paramètres clés des systèmes chaotiques, notamment la dimension de corrélation, le spectre de Lyapunov et la dimension de Lyapunov, sont calculés à partir du clutter de mer réel, et on constate qu'ils sont compatibles avec une interprétation basée sur la théorie du chaos. On vérifie le caractère déterministe du clutter de mer en établissant un prédicteur non linéaire à une étape. Deux approches différentes sont mises en application, une technique linéaire locale et un réseau neuronal à fonction de base radiale (FBR). Une bonne performance est obtenue avec une erreur quadratique moyenne (EQM) égale approximativement à 0,0032, mesurée entre les séries chronologiques prévues et les séries réelles normalisées.

McDonald, M.K. 2001. Clutter de mer chaotique : état actuel et application aux systèmes radar aéroportés. DREO 2001-114. Centre de recherches pour la défense Ottawa.

Table of contents

List of figures

List of tables

Acknowledgements

The contribution of Dr. Leung's group at the University of Calgary in performing analysis on the AN/APS-506 sea clutter data is gratefully acknowledged.

This page intentionally left blank.

1. Introduction

The study of radar detection in clutter has traditionally relied on the application of stochastic theory to the development of target detection schemes. In theory, modelling sea clutter with an appropriate statistical distribution allows the calculation of the detection probability for a specified false alarm rate. Early studies of sea clutter returns from low resolution radars were quite successful in applying the Guassian probability distribution to the detection problem; the success of this approach made intuitive sense as the total return from any resolution cell (nominally the area defined by the beamwidth and range resolution of the radar) could be viewed as the sum of the many scatterers within it; for a very large numbers of scatterers the application of the central limit theorem (CLT) will result in the aforementioned Guassian distribution. The theory surrounding the application of the Guassian distribution is well developed, Skolnik [1], for example, provides a good introduction.

Since the strength of clutter returns is directly proportional to the cell area being viewed, it was anticipated that improving the range resolution of radars systems (i.e. smaller resolution cell areas) would result in a corresponding improvement in detection capability. Unfortunately, this did not prove necessarily true as an increasingly impulsive or spiky character was observed to develop in the clutter returns as the cell size was decreased. The observed breakdown of the Guassian behaviour is almost certainly the result of bunching of scatters due to correlations in the underlying sea surface structure. To overcome the aforementioned shortcomings, several other distributions have been suggested as models for the statistics of sea clutter returns. Two of the most favourable candidates currently being considered are the K distribution and spherically invariant random processes (SIRP), the former being applied to envelope detection processes while the latter is applied to coherent detection (SIRP can be shown to reduce to the K distribution when amplitude envelope detection is imposed). The theory surrounding the application of these distributions to the target detection problem is ongoing and a large body of literature exists (see for example [2,3,4]).

The common element in all the above approaches is that the clutter returns are assumed to be stochastic processes with infinite degrees of freedom, or at the very least, processes that have such a large number of degrees of freedom that the only practical approach is to model them as stochastic processes. Qualitatively a stochastic interpretation appears to be consistent with the observed spectrums of real clutter returns, which are typically highly irregular in character and have continuous broadband spectrums reminiscent of broadband noise. Figure 1a shows an example of real clutter returns measured using the high resolution AN/APS-506 maritime surveillance radar. The spectrum of the same signal is shown in figure 1b. The irregular nature of the return and the continuous broadband nature of the spectrum are readily apparent. The measured probability distribution is also shown.

In contrast to the focus on stochastic methods it has recently been suggested that sea clutter returns can be modelled using chaos theory [5]. Chaotic systems are non-linear dynamic systems with a relatively small number of degrees of freedoms. The last thirty years has seen a growth in the understanding of these deterministic dynamic systems that have the unusual property of displaying seemingly random behaviour.

This first section of this report reviews the general characteristics of non-linear dynamic systems. This section is followed by brief introduction to chaotic systems and some of the invariant measures and properties associated with them. The next section very briefly introduces neural networks in preparation for the discussion of past attempts to model sea clutter as a chaotic systems which is presented in the succeeding section. The final section summarizes the results of recent studies undertaken by DREO and the University of Calgary to investigate the chaotic behaviour of sea clutter returns collected from moving airborne platform.

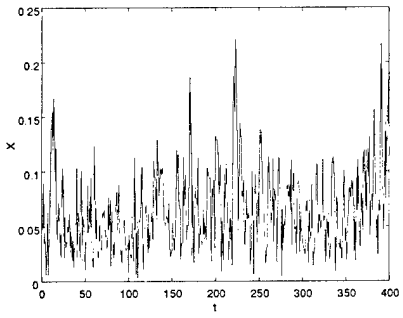

(a)

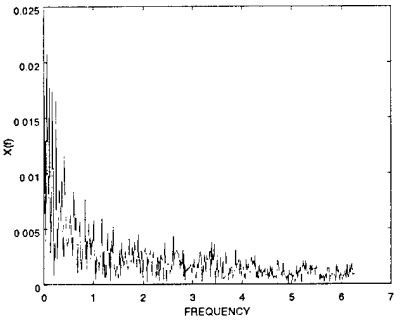

(b)

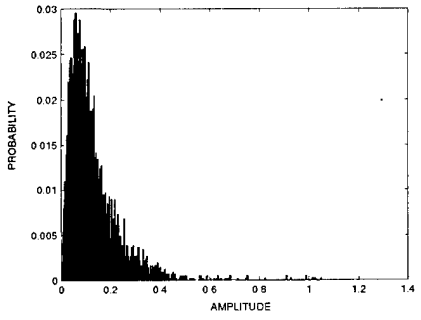

(c)

Figure 1. *Sea clutter returns from AN/APS-506 radar (a) Time series of amplitude. (b) Spectrum of amplitude. (c) Probability distribution of amplitude.*

2. Non-Linear Dynamic Systems

To understand the material presented in this report it is necessary to briefly review non-linear dynamic systems. The general form of a dynamic system can be written as

$$\frac{dx}{dt} = f(x) \qquad (1)$$

for an nth-order autonomous dynamical system and

$$\frac{dx}{dt} = f(x,t) \quad (2)$$

for the nth-order nonautonomous dynamical system where $x(t) \in R^n$ is the state at time t, $f : R^n \rightarrow R^n$ is the vector field and R^n is the state space. This form of definition permits the existence of a wide variety of systems. Parker and Chua [6] provide a useful tutorial describing the behaviour of a variety of non-linear systems. They identify a number of different types of systems admitting equilibrium point, periodic and quasi-periodic solutions.

It is clear without further consideration that any solution of the above dynamic system that tends to an equilibrium point would not be representative of the irregular nature of the clutter response shown in figure 1. In addition, examination of the temporal and spectral characteristics of systems with periodic and quasi-periodic solutions shows that they are also poor models for real clutter returns. This point is clarified below by examining the temporal and spectral properties of examples of the latter two types of systems. Parker and Chua's work [6] uses van der Pol's equation in their examples, for convenience the same dynamic system will be presented here. Readers requiring a more in depth analysis are referred back to the aforementioned paper and references therein.

A classic example of a limit cycle in a periodic system is given by van der Pol's equation

$$\frac{dx}{dt} = y, \qquad (3)$$

$$\frac{dy}{dt} = (1-x^2)y - x. \qquad (4)$$

The steady state solution for this system is shown in figure 2a; figures 2b and 2c show the x component of the corresponding temporal waveform and spectrum, respectively. Comparing figure 2 for the periodic solution of van der Pol's with the real returns in figure 1, it is immediately clear that the temporal behaviour of real clutter returns is much more irregular than that associated with the periodic solution. Figure 2c shows that the spectrum of the periodic solution is composed of discrete components, quite different from the broad continuous spectrum of the clutter in figure 1b.

Adding a forcing term to Van der Pol's equation forms an example of a quasi-periodic system,

$$\frac{dx}{dt} = y, \qquad (5)$$

$$\frac{dy}{dt} = (1-x^2)y - x + A\cos 2\pi(\frac{t}{T_2}), \qquad (6)$$

where the system is assumed to have a natural unforced period, T_1, and a forcing term with a period T_2 and an amplitude A.

The solution to this system can either synchronize with some multiple of the forcing period, T_2, giving the periodic solution, or as an intermediate case neither T_1 nor T_2 will dominate and quasi-periodic behaviour occurs. Figure 3 illustrates an example of a quasi-periodic solution for this equation. Comparing figure 1a of real sea clutter returns with figure 3b it is again apparent that while the temporal behaviour of the x component of the system is more strongly modulated for the quasi-periodic solution (in comparison with the periodic example of figure 2b) with both amplitude and frequency modulation present, the overall behaviour is still far too regular to serve as a reasonable model of clutter returns. In addition, the spectrum of the forced van der Pol's system is composed of tightly spaced sidebands of discrete frequencies centred on the natural frequencies of the unforced system, quite different from the spectrum of clutter returns in figure 1b. It should be emphasised that while the above two examples are both based on the van der Pol's equations, the qualitative characteristics described above, namely the regular temporal behaviour and the discrete spectrum components, will in general hold true for other periodic and quasi-periodic solutions.

All the solutions discussed so far, namely the equilibrium point, periodic and quasi-periodic, possess a fundamental limit set and while the existence of a steady state limit is obvious for an equilibrium point solution it is also readily apparent in the state diagram of figure 2a for the periodic system. The existence of a limit set is somewhat less obvious for the quasi-periodic solution but can be readily shown by diffeomorphically copying the trajectory into the S by S torus space of the two base frequencies. The trajectory repeatedly passes arbitrarily close to every point on the torus, which then defines the limit set of the quasi-periodic solution. Figure 4 illustrates this concept more clearly. The attracting limit set is often simply referred to as the attractor.

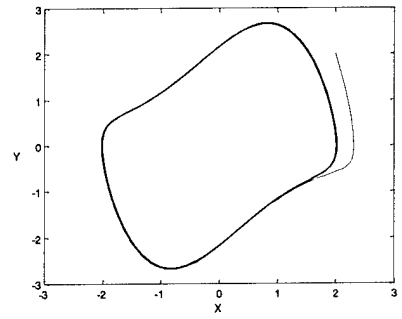

(a)

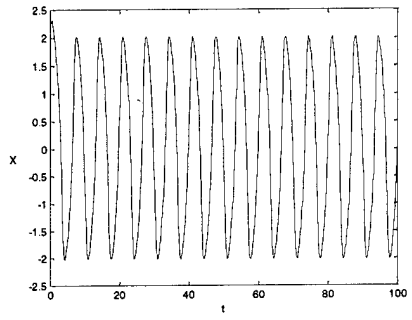

(b)

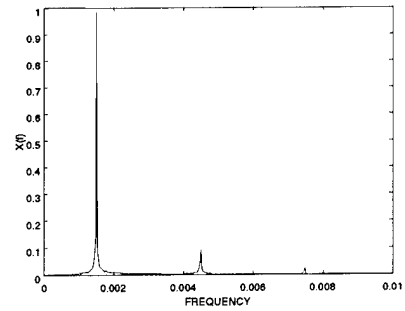

(c)

Figure 2: *Periodic behaviour of van der Pol equation. (a) Trajectory. (b)Time series of x component. (c) Spectrum of first component.*

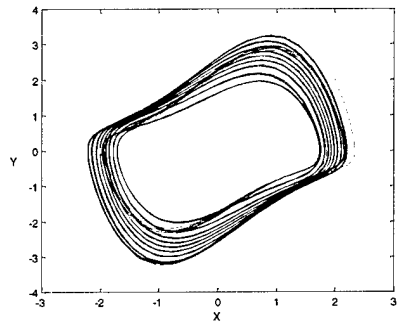

(a)

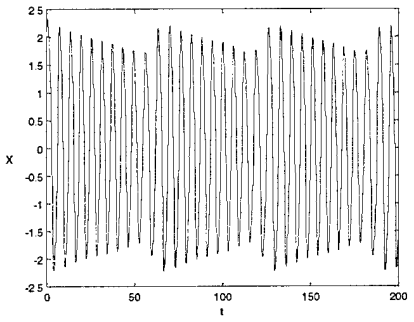

(b)

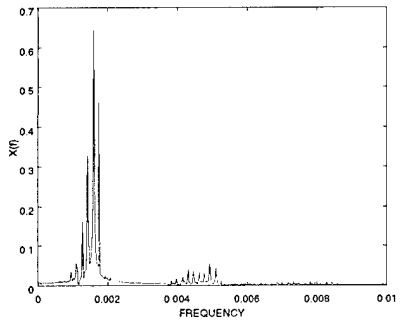

(c)

Figure 3: *Quasi-periodic behaviour of van der Pol equation for A=0.5 and* $T_2 = \frac{2\pi}{1.1}$. *(a) Trajectory. (b) Time series of x component. (c) Spectrum of first component.*

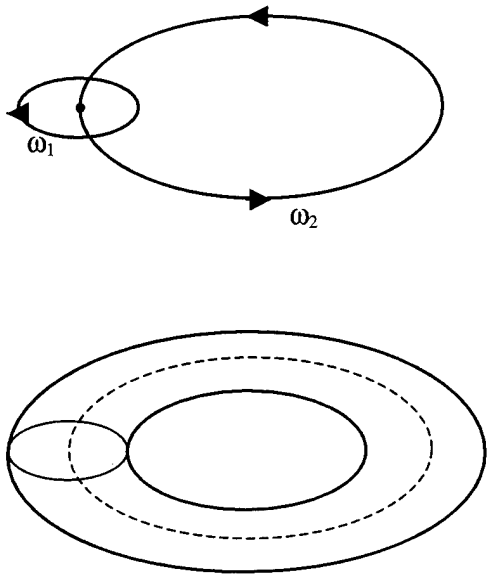

Figure 4. *Diffeomorphic copy of trajectory of two periodic system (fig. 3a) into S by S torus space. Each dimension S represents one of the base frequencies of the quasi-periodic system. Trajectory passes arbitrarily close to each point on torus.*

3. Chaotic Dynamic Systems

Unlike the dynamic systems described above, chaotic systems possess the unusual property of displaying apparently noise-like behaviour. This noise-like behaviour is the result of the sensitive dependence of a chaotic system to its initial conditions. A chaotic system is a deterministic system and in theory its future behaviour can be predicted provided its initial state is precisely known. In practice however, it is impossible to measure any initial state exactly; therefore in a chaotic system any two measured initial states that are arbitrarily close to each other will, with time, diverge at an exponential rate until they are effectively uncorrelated. The rate at which they diverge will depend on the particular system but the inherent unpredictability of these systems gives rise to their noise-like character.

Chaotic systems typically display a temporal behaviour that appears qualitatively quite random or irregular and unlike periodic and quasi-periodic solutions, the spectrum of a chaotic solution is continuous and broadband. Both these qualities are partial prerequisites for any dynamic system proposed as a model of sea returns. Figure 5 illustrates an example of a solution of the chaotic system represented by Duffing's equation

$$\frac{d^2y}{dt} = -\delta\frac{dy}{dt} + y - y^3 + \gamma\cos(\omega t). \quad (7)$$

where δ is the damping inherent in the system, and ω and γ are the angular frequency and amplitude, respectively, of the forcing term. The irregular nature of the solution and the broad flat spectrum associated with it are readily apparent. In addition, the solution is clearly bounded, consistent with real sea clutter returns. The object on which the trajectories of a chaotic system accumulate is termed a strange attractor in contrast to the attractor of periodic and quasi-periodic solutions. The strange attractor concept is an important one in chaos theory and will be discussed further in the following sections.

If it can be shown that sea clutter is in fact a chaotic system, and the function describing it can somehow be determined, then the deterministic nature of a chaotic solution should prove more informative then the stochastic approach; improved modelling and detection capabilities should result. While the above discussion is illustrative of some of the qualitative similarities between sea clutter and chaotic systems, it is by no means certain that sea clutter can be modelled as a chaotic process. Before moving on to the issue of applying chaos theory to sea clutter it is necessary to briefly introduce and discuss some basic concepts that will arise in the ensuing discussions.

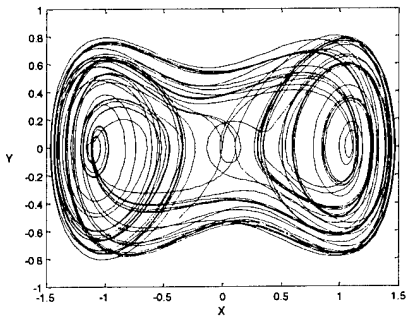

(a)

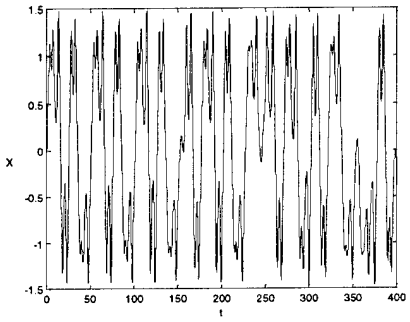

(b)

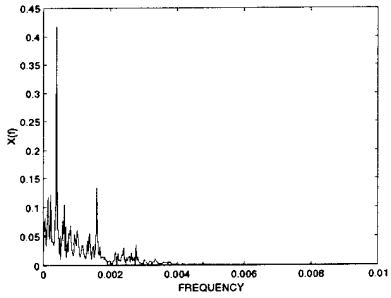

(c)

Figure 5: *Chaotic behaviour of Duffing's equation δ = 0.25, γ=0.3, ω=1.0 (a) Trajectory. (b) Time series of x component. (c) Spectrum of first component.*

3.1 Attractor Dimension

One invariant measure fundamental to the classification of attractors is dimension. An attractor is defined as being n-dimensional if in the neighbourhood of every point it looks like an open subset of the state space of dimension n. Figures 2 and 3 respectively present the examples of periodic and quasi-periodic solutions discussed earlier. We see that the periodic attractor has a dimension of one since it can diffeomorphically mapped to a subset of R^1. The quasi-periodic case is two dimensional as was clearly seen through the diffeomorphic mapping of the trajectory onto a two dimensional torus discussed earlier. An equilibrium solution would have zero dimension. Strange attractors differ from the above in that they do not have an integer dimension; the dimension associated with them is fractal. A wide variety of definitions of dimension exist for strange attractors, the interested reader is referred to Parker and Chua's tutorial [6]; for the purposes of this report we concentrate on correlation dimension, the most commonly used measure of dimension in papers on the application of chaotic theory to sea clutter.

In its essence, correlation dimension is a measure of the correlation between an arbitrary point on the attractor manifold and its surrounding points averaged over all locations on the manifold. Probably the easiest way to clarify this description is to examine one of the earliest algorithms for calculating it as presented by Grassberger and Procaccia [7]. The first step is to consider a set of N points, identified as x_j with $j = 1, N$ on an attractor embedded in a phase space of dimension n. We now define a function, referred to as the correlation integral of the attractor, as follows

$$C(r) = \lim_{N\to\infty} \frac{1}{N^2} \sum_{i,j=1}^{N} \theta(r - |x_i - x_j|), \qquad (8)$$

where θ is the Heaviside function with $\theta = 0$ if $x < 0$ and $\theta = 1$ if $x > 0$. The norm $|x_i - x_j|$ is either the maximum norm or Euclidean norm and r is a prescribed distance from the test point x_i. This definition of $C(r)$ illustrates the correlational nature of the dimension. It can be shown that [7]

$$C(r) \approx r^{D_c}, \qquad (9)$$

where D_c is the correlation dimension and r is reasonably small. This power law relationship can be exploited to determine D_c by plotting $\log C(r)$ versus $\log r$. In the region where the power law holds, the slope of the line will be constant and equal to the correlation dimension. Typically curves are plotted for increasingly large embedding dimensions until the estimates from the slopes of each curve converge indicating that a sufficiently large embedding dimension (embedding dimension is discussed further in section 3.4) is being used. This process allows both the correlation dimension and minimum required embedding dimension to be determined. The process is also a useful diagnostic for identifying systems which are not chaotic in nature: if the value for correlation dimensions does not converge with

increasing imbedding dimension this is indicative of a process which is truly random or deterministic with very high degrees of freedom. Clearly a chaotic system would be a poor choice as model under these circumstances.

The power law described above holds true only for small r, in theory the smaller r utilised the more accurately D_c can be calculated, however this improvement is offset by the limited size of any data set. Clearly if r is made very small then very few data points will lie within the spherical region of radius r, under these conditions the calculation of D_c will not be very accurate. It is necessary to ensure that a sufficiently large data set is available so that a sufficiently small r may be used in the calculation.

3.2 Lyapunov Spectrum

As discussed above, one of the most fundamental properties of a chaotic system is its sensitivity to the initial starting conditions. Any two measured initial states that are arbitrarily close to each other will, with time, diverge exponentially from each other until they are effectively uncorrelated. The rate at which they diverge will depend on the particular system. This raises the important question of how to define and quantify a parameter, which characterises the evolution of the trajectories.

A useful starting point to consider is the simpler case of equilibrium point solutions. Denoting the equilibrium point as x_{eq} and linearising the function f, introduced in equations (1) and (2), we write the formula defining the time evolution of perturbations about the equilibrium point as

$$\frac{d(\delta x)}{dt} = Df(x_{eq})\delta x(t), \qquad (10)$$

where D is the Jacobian of the system. The trajectory with initial condition $x_{eq} + \delta x_0$ is given to the first order by

$$\phi(x_{eq} + \delta x_0) = x + \delta x(t), \qquad (11)$$

substituting in (10) we obtain

$$\begin{aligned}\phi(x_{eq} + \delta x_0) &= x_{eq} + e^{Df(x_{eq})t}\delta x_0 \\ &= x_{eq} + c_1\eta_1 e^{\lambda_1 t} + \ldots + c_n\eta_n e^{\lambda_n t},\end{aligned} \qquad (12)$$

where λ_i and η_i are the eigenvalues and eigenvectors, respectively, of $Df(x_{eq})$. c_i is a scalar constant chosen to match initial conditions. It is clear from the structure of equation (12) that if $RE[\lambda_i] < 0$ for all i then the equilibrium point will be stable as all perturbations will tend to zero as $t \to \infty$.

The same approach can be applied to the periodic solutions. In this case use is made of the Poincaré map which is essentially a method of representing a trajectory by sampling it at constant time intervals, typically the natural frequency of the system. As such the Poincaré map of a periodic solution corresponds to a point, denoted x^*. The linear discrete time evolution of a perturbation about this point is given by

$$\delta x_{k+1} = DP(x^*)\delta x_k . \quad (13)$$

In a directly analogous manner to the equilibrium point solution we can derive the eigenvalues (m_i) and eigenvectors (η_i) of $DP(x^*)$. The eigenvalues (m_i) are called characteristic multipliers and determine the contraction and expansion around x^* for each sampling interval.

The equivalent desired invariant for a chaotic system is the Lyapunov exponents, which are a generalization of the characteristic multipliers, specifically the Lyapunov exponents are defined as [6]

$$\lambda_i = \lim_{t\to\infty} \frac{1}{t} \ln | m_i(t) | . \quad (14)$$

The entire set of Lyapunov exponents associated with a dynamic system is referred to as the Lyapunov spectrum. Using the concept of Lyapunov exponents we can define additional requirements that must be met for a system to have the potential of being considered a bounded chaotic solution. It can be shown that at least one Lyapunov exponent must be equal to zero; a condition which is true for any bounded attractor of an autonomous system. In addition, if the system is to show the sensitive dependence to initial conditions that is characteristic of a chaotic system, at least one Lyapunov exponent must be greater than zero [8]. This condition makes intuitive sense, as initial condition sensitivity is a property of an expanding flow. This property must be met for a system to be considered chaotic. If the solution is to be bounded, a requirement for a real dissipative process such as a sea clutter, it is also necessary that the sum of the exponents be less than zero [6].

A by-product of the Lyapunov spectrum is the Lyapunov dimension, $D_{Lyapunov}$, defined by [9]

$$D_{Lyapunov} = K + \frac{\sum_{i=1}^{K} \lambda_i}{| \lambda_{K+1} |}, \quad (15)$$

where the λ_i are arranged in descending order and the integer K satisfies the conditions

$$\sum_{i=1}^{K} \lambda_i > 0, \quad (16)$$

$$\sum_{i=1}^{K+1} \lambda_i < 0. \qquad (17)$$

If a dynamical system is chaotic it must have a Lyapunov dimension that is close to the calculated correlation dimension, comparison of these two independently calculated values provides a useful crosscheck of the algorithms used to calculate each.

3.3 Kolmogorov entropy

The Kolmogorov entropy, h_k, is a generalization of Shannon's entropy to dynamical systems. It provides a measure of the rate of change in our ability to specify the microscopic state of a chaotic system as time progresses. This parameter and the methods of calculating it are discussed in more detail in other papers; see Haykin [10] and references therein. The Kolmogorov entropy and the sum of the positive Lyapunov exponents should be equal

i.e. $$h_K = \sum_{\lambda_i > 0} \lambda_i . \qquad (18)$$

Comparing the sum of the calculated Lyapunov exponents with the independently calculated Kolmogorov entropy provides a useful crosscheck of the algorithms used to calculate each.

3.4 Reconstructing Attractors

In a real or experimental setting it is typically impractical or impossible to collect information on all the state variables. At first glance this restriction would seem to prohibit the reconstruction of the underlying attractor, however, it has been shown that it is possible to reconstruct the attractor of a chaotic process using only one component of the state. The approach utilised employs a time delay embedding technique and was first put on firm theoretical footing by Takens [11]. It is subsequently referred to as Takens' embedding theorem. The application of this theorem begins by formulating the d_E dimensional reconstruction vector

$$r(m) = [y(m), y(m-\tau), ..., y(m-(d_E-1)\tau], \quad (19)$$

where d_E is the embedding dimension, τ is the normalized embedding delay and $y(m)$ is an observable component which is related to the state vector $x(m)$ by

$$y(m) = g(x(m)), \qquad (20)$$

with $g(\bullet)$ a smooth scalar function. A sequence of such vectors can be generated by advancing through the index m. Takens showed that if the strange attractor is a D_c dimensional object, an embedding dimension d_E equal to $2D_c + 1$ will allow

reconstruction of the underlying attractor. This requirement is only a sufficient condition, however, and a suitable d_E may be found to lie within the range $[D_c, 2D_c + 1]$. Essentially this says that a reconstruction vector, $r(m)$, of suitable dimension d_E will uniquely determine the next vector $r(m+\tau)$. In practical terms this can be exploited by building a sequence of reconstruction vectors of the observable component, if these vectors are of sufficient embedding dimensions they will successfully define the attractor and can be used to develop a predictive model of the chaotic system. As an example, the reconstruction vectors could be used to train a neural network to approximate the dynamic Ψ which connects the vectors $r(m)$ and $r(m+\tau)$, i.e.

$$r(m+\tau) = \Psi(r(m)). \quad (21)$$

The choice of time delay, τ, requires some care. If τ is too small then $r(m)$ and $r(m+\tau)$ will be too close and they will not be independent, the reconstructed attractor will then be restricted to the diagonal of the reconstruction space. If τ is too large then $r(m)$ and $r(m+\tau)$ are uncorrelated and the structure of the attractor is lost.

4. Neural Networks

To exploit the chaotic nature of a system a method is required for approximating its transfer function. Neural networks possess the ability to approximate any continuous function by adaptation through training with a sample set of data from the real system. In the papers discussed in this report two different types of neural nets are considered, namely the Radial Basis Function neural net and the MultiLayer Perceptron neural net. While it is beyond the scope of this report to describe these two different approaches in detail the basic structure of each as well as its advantages or disadvantages is summarized below. The interested reader is referred to Haykin [12] for a more detailed discussion.

4.1 Radial Basis Function (RBF)

The structure of the RBF neural net is shown in figure 6. It is composed of a layer of input nodes connected to a hidden layer of computing nodes by linear synaptic connections. The hidden layer is in turn coupled to the output layer by non-linear synaptic connections. The RBF network possesses an on-line learning ability, a property essential for any real time signal processing application. It also possesses an inherent regularisation ability that makes it a robust technique for dealing with ill posed problems such as model fitting from noisy data.

4.2 MultiLayer Preception (MLP)

The structure of a MLP neural net is shown in figure 7. It is composed of a layer of input nodes connected to two or more layers of hidden neurons. Typically the computation nodes of the hidden layers are non-linear and the output layer is linear. The MLP neural net is trained using a back-propagation algorithm that adjusts the weights of the interconnecting synapses. The back-propagation algorithm is known to have slow convergence and is not suitable for a real time signal processing application.

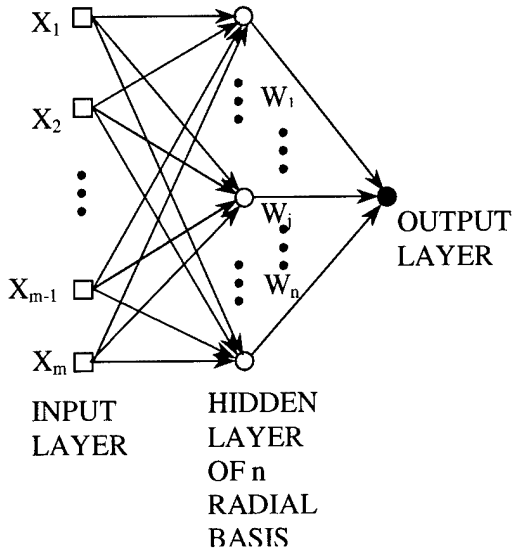

Figure 6. *Radial basis function neural network.*

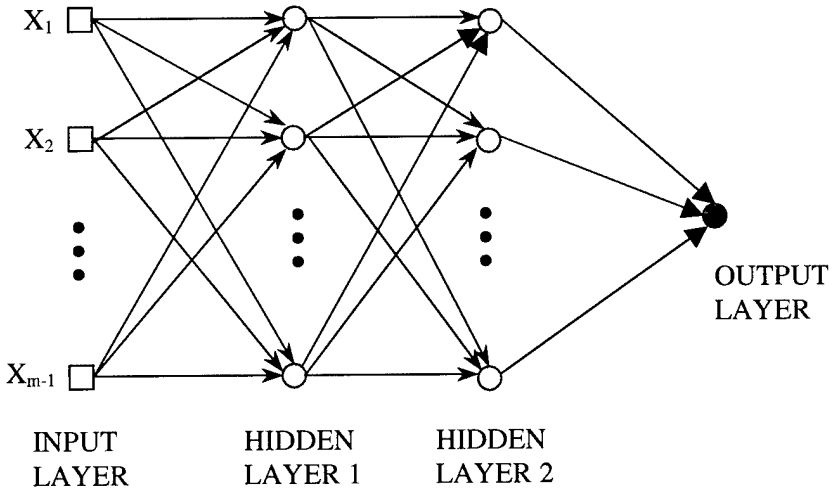

Figure 7. *MulitLayer preceptron neural network.*

5. Modelling Sea Clutter as a Chaotic System

As discussed above the potential for applying chaos theory to the modelling of sea clutter returns is suggested by the qualitatively similar appearance of temporal returns and spectrums from sea clutter and chaotic systems. The motivation for doing so lies in the fact that a deterministic model of sea clutter, if successful, will significantly reduce the degrees of freedom and should result in improved detection performance. A historical review of the application of chaos theory to sea clutter is given below, culminating with the current state of research.

Leung and Haykin [5] were the first to suggest the existence of a radar clutter attractor. They used low resolution (i.e. 30 m range resolution) data collected using the IPIX radar in the coastal location of Cape Bonavista, Newfoundland. The radar was operated in a 'staring mode' to collect returns from the ocean surface along a radial line. This first attempt at establishing the existence of a radar clutter attractor was crude; Leung and Haykin employed relatively short time series of data, only 2000 points, in the calculation of the correlation coefficient. In addition they chose the time delay used for the embedding by trial and error, finally settling on a value they felt gave embedding co-ordinates that appeared 'reasonably independent.' In their paper they adopt the Grassberger and Procaccia algorithm for calculating the correlation dimension [7]. From their analysis they concluded that the correlation dimension of the attractor has a value lying between 6.4 and 6.7. Because of the short time series and subjective choice of embedding delay their results were far from conclusive but they did open up the tantalising prospect of the existence of a radar attractor.

Three years later Leung and Lo [13] published a paper further studying the chaotic nature of sea clutter and also attempting limited detection of ice 'growlers' (small fragments of icebergs) in sea clutter. They again utilise data collected with the IPIX radar at the Cape Bonavista, Newfoundland site and attempt to address some of the shortcomings of the earlier paper by Leung and Haykin [5]. In particular, the length of the time series used to calculate the correlation coefficient has been increased to 20000 samples with the expectation of improved accuracy. They have also adopted a more objective method for determining the required time delay between embedding samples, specifically, they use the first zero-crossing point of the autocorrelation function of the time series as the normalized embedding delay, τ.

Using the method of Grassberger and Procaccia [7], they analysis four data sets and report correlation dimensions ranging from 5.8 to 7.2. Because of the inaccuracy of their calculations they are unable to speculate on any relationship between the correlation dimension and the physical properties of sea surface producing the clutter returns such as wave height or wind speed.

For the first time Leung and Lo develop a non-linear predictive model of the sea clutter returns using a neural networks trained with sample data from the real system to approximate the continuous function. They chose to implement an RBF neural network [12]. Their choice of the RBF neural net was partly motivated by its on-line learning ability and inherent regularisation.

After training the RBF network with a 2000 point set they undertake to perform one step predictions of the system state. This corresponds to the mapping

$$x(t+\tau) = f(x(t)), \qquad (22)$$

where $x(t+\tau)$ is the predicted state vector at the next time step, $x(t)$ is the current state vector and f is the mapping function to be approximated by the neural net. Since we are working with the embedded reconstruction of the attractor manifold $x(t)$ will correspond to the d_E dimensional vector corresponding to the current time step, the function f predicts the first element of the d_E dimensional vector corresponding to the next time step. This operation is performed for a range of embedding dimensions (corresponding to the number of nodes in the input layer) from 2 to 22 and for each fixed embedding dimension the number of hidden nodes is determined by trial and error i.e. by adjusting the number of hidden nodes until a prediction error minimum was achieved. Leung and Ho compare the prediction errors that resulted from using the RBF neural net (assuming sufficient embedding dimension has been reached) against those that occurred when a standard linear predictor was used; they conclude that a 2-5 dB improvement is achieved when the neural net that was used. The results from the RBF predictor also indicate the optimum embedding dimension. Fairly distinct minimums are visible in the plots of prediction error versus embedding dimension for the chaotic detector but not for the linear detector. The presence of these minimums is expected for chaotic systems but not for linear detectors.

Leung and Lo use then use the trained RBF predictor to perform detection on small iceberg fragments called growlers. The principle behind the chaotic detection method is simple and based on the comparison of prediction errors. Since the RBF neural net has been trained using data in which the H_0 hypothesis is correct, i.e. no target present, then a prediction $\hat{x}(t+\tau \mid H_0)$ will be optimum in a mean squares sense while a prediction $\hat{x}(t+\tau \mid H_1)$ will not. The prediction error can be calculated as

$$\varepsilon = \hat{x}(t+\tau) - x(t+\tau). \qquad (23)$$

A prediction error threshold can then be defined to predict the presence of a target as follows

$$H_1 : if \ \varepsilon > \eta,$$

$$H_0 : if \ \varepsilon < \eta.$$

Leung and Lo average the one step prediction error from multiple predictions and chose the optimum threshold, η, using a maximum likelihood criteria. This criteria leads to a probability of false alarm (PFA) that would be unacceptably high for any real operating radar, nevertheless, the comparison of the receiver operating characteristics of the chaos based detector against two standard detectors, namely the amplitude and AR-based adaptive detector, suggests that an improvement in detection performance does occur for chaotic

detection. Whether the degree of improvement is significant for small PFA's on the order of 10^{-4} is not discussed.

In 1994, Blacknell and Oliver undertook their own examination of the chaotic behaviour of sea clutter returns in which they raise concerns about the existence of a sea clutter attractor [14]. In their analysis real time series of data are compared with artificially generated 'random' times series. To form the real time series they incoherently add the measured range lines returns from over 250 pulses to form a single range line from which the multiplicative speckle noise has been removed. Consecutive range lines are combined in a two dimensional array with one axis representing time and the other range. The fluctuations across the two dimensional array are well modelled by a correlated gamma distribution. The simulated image is generated by measuring the autocorrelation function of the above 'real data' array and imposing it on a two dimensional array of gamma distributed noise generated using an appropriate 'random' number generator.

Blacknell and Oliver calculate the correlation dimension of both the real and simulated data. Since they only have 224 time samples in each range bin they combine data from 10 adjacent line bins to increase the accuracy of the correlation coefficient calculation. The results of their calculations on the real data indicate that the slopes of the $\log(C(r))$ versus $\log(r)$ plots become constant with increasing embedding dimension for a correlation dimension in the range from 3 to 4. However when the analysis was repeated with the simulated data the same behaviour was observed, that is the correlation dimension becomes constant at higher embedding dimensions. If the simulated data is truly a stochastic process it should have infinite degrees of freedom; as the embedding dimension was increased the calculated correlation dimension should have continued to increase to fill the available phase space. Blacknell and Oliver suggest that this unexpected result 'raises a general doubt about the practicality of the correlation dimension measurement technique' and by implication questions the results of the earlier papers by Leung and Haykin, and Leung and Lo, which rely on the calculation of a fractal correlation coefficient as their primary evidence that a chaotic sea clutter attractor exists. It should be recognised that the time series Black and Oliver used to calculate their correlation coefficients is only 2240 time samples long, this is roughly the same as the 2000 sample time series used by Leung and Haykin [5] in their initial paper, but far short of the 20000 samples used by Leung and Lo [13]. The accuracy of Blacknell and Oliver's calculations should be treated with caution: they recognise this shortcoming but they also question whether a sea clutter attractor will be stationary over the length of time required to form the necessary length of time series. It is also unclear whether their observation of finite embedding dimension for the simulated 'random' time might be caused by the shortness of their time series. Another possible explanation for the finite correlation dimension of the 'random' process may lie in the fact that random number generators implemented by a computer are in fact fully deterministic. Although with a very long period of repeatability, 'noise' generated by this method may in fact have a finite attractor associated with it.

Blacknell and Oliver also point out that presence of correlation in the time series will delay the convergence of the correlation dimension estimate, they have not taken any special care to ascertain the required embedding delay in their analysis, simply using the sampling period of the original data.

This is not likely to be a significant concern for the Leung and Lo paper where the autocorrelation method was used to calculate the embedding time delay [13].

Blacknell and Oliver also studied the effect of noise in the time series on the correlation dimension estimates. They generated a time series of 1500 samples at 0.1 s seconds intervals from a Lorentz system and added Guassian 'noise' generated using a random number generator. Their experiment seems to indicate that the added noise has the greatest effect on the slope estimates from the $\log(C(r))$ versus $\log(r)$ plot at small values of r. This makes intuitive sense as the noise distribution is weighted more heavily to the smaller amplitudes. As r is increased the percentage of the noise contribution to the distribution of lengths is smaller and the slope estimate becomes more accurate. However, as mentioned earlier the linear power law relationship is really defined for the limit as $r \rightarrow 0$, and as such it becomes less accurate with increasing r. Therefore measurement of the correlation dimension per Grassberger and Procaccia is limited for small r by noise and for large r by fundamental considerations. Blacknell and Oliver's results suggest that a minimum signal to noise ratio (SNR) of 18 dB is required to allow identification of a chaotic signal in noise using the above approach.

Leung [15] re-examines the issue of chaotic detection in an oceanic environment using additional data sets drawn from the same large database (Cape Bonavista, June 1989) used in earlier 1993 paper by Leung and Lo [13]. In this 1995 paper, Leung calculates the correlation coefficients corresponding to four different scenes and shows that correlation coefficients for scenes with targets are lower then pure clutter scenes. He qualitatively explains this phenomenon in terms of the high level of geometric regularity associated with targets present in the scene. While the difference in correlation coefficient is of theoretical interest it is not a practical method for use in real time radar systems due to the large number of points that are needed to perform the analysis. As discussed above, the 1993 paper examined the use of nonlinear prediction to detect targets in clutter; Leung again uses this approach to detect the targets present in each of the four data sets examined in the 1995 paper. Unlike the 1993 paper where receiver operating curves (ROC) are presented, the 1995 paper presents the actual histograms of the prediction errors from sets with and without targets. His results demonstrate that the average prediction errors associated with the sets containing a target are significantly larger than those associated with sets containing only clutter. This was to be expected as the neural network based non-linear predictor was trained using 'clutter only' data sets. Unfortunately Leung does not present results obtained using other more common detection methods or provide any quantitative analysis of the prediction performance for practical false alarm rates (e.g. 10^{-4}), as such the applicability of the method to real surveillance systems is unclear.

Haykin and Li [16] readdress the detection in chaos issue in 1995 with an extensive analysis of the chaotic properties of sea clutter. Until this point the evidence supporting the description of sea clutter as a chaotic process has been primarily limited to the calculation of a fractal correlation coefficient. This is a necessary but insufficient property for identifying a chaotic property. Indeed given the broad ranges of the calculated correlation coefficients it is difficult to evaluate the absolute accuracy of the algorithms used to compute the correlation coefficient from the time series. Haykin and Li recognise the limitations of using only correlation dimension as a discriminator and reference a counter example from studies that show coloured noise can also exhibit a finite correlation dimension [17]. Building on

Newhouse's definition of a chaotic system [18], they offer their own definition of a chaotic system as: "A bounded deterministic dynamical system with at least one positive Lyapunov exponent is a chaotic system. A chaotic signal is an observation of the system."

Haykin and Li examine three essential elements of their definition:

1) The boundedness of sea clutter returns.

2) Deterministic character of sea clutter returns.

3) Existence of a positive Lyapunov exponent

Since the signal in question arises from reflection and scattering of a finite transmitted signal the boundedness of the sea clutter returns is readily apparent.

They test the deterministic property of the system by examining its dimension and its predictability. Generally speaking a deterministic system has finite dimension and by definition a deterministic system is predictable, provided the underlying model for the system can be found.

As with the other papers they focus on the correlation dimension as an invariant measure of the system. They utilise the box counting algorithm of Pineda and Sommerer [19], which is computationally more efficient then the original algorithm of Grassberger and Procaccia [7], and consider the relationship derived by Eckmann and Ruelle for the limits applying to the required data set size

$$D_c \leq \frac{2\log N_{total}}{\log(\frac{1}{\rho})}, \qquad (24)$$

where $\rho = \frac{\varepsilon}{L} << 1$, L is the diameter of the reconstructed attractor and ε is maximum mutual distance [20]. This relationship provides a lower bound on the size of the data set, N_{total} required to estimate a correlation dimension D_c. Data from three separate locations, Cape Bonavista, Newfoundland, Dartmouth, Nova Scotia and a site overlooking Lake Ontario at Stony Creek, Ontario is used in this study. Each data set consists of at least 40,000 points and the combined database covers a broad range of wind speeds and sea states. According to the Eckmann and Ruelle limit, the maximum correlation coefficient that can be estimated for a 40,000 point set is $D_c \leq 9.4$. In identical fashion to that described above they calculate the correlation dimension for increasing embedding dimension until convergence of the calculated correlation dimension is observed. To determine the appropriate time delay between embedding samples they use the method of mutual information content (MI). Their analysis gives fractal correlation dimensions varying from 7-9 across the data sets. No appreciable pattern of variation according to sea state or location is observed. Haykin and Li perform additional calculations to test the reliability of estimates; they repeat the calculation of the correlation coefficients using a variety of different lengths for the data sets and observe

that for data sets longer than 10,000 samples the calculated correlation coefficients appear stable.

To test the influence of noise on the calculated correlation coefficients they chose two of the data sets for further processing. In particular they chose sets drawn from near and far range returns, the near range set possessing a much larger clutter to noise ratio (CNR) than the far range set. A simple three point smoothing filter (lowpass filter) is applied to the raw sea clutter data. When the correlation dimension procedure is repeated on the filtered sets essentially no difference is observed in the rate at which the correlation dimension of the filtered and unfiltered high CNR set converges to a stable value with increasing correlation. In contrast, the unfiltered low CNR set demonstrates no convergence of the calculated correlation coefficient, after filtering however, the correlation dimension demonstrates a good convergence with increased embedding dimension, similar to the behaviour of the high CNR set. This result makes intuitive sense as a random process, which possesses infinite (or at least very large) degrees of freedom should not converge to a finite correlation dimension. Once the dominating effect of the noise is removed from the data set through filtering, the chaotic character of the data is observed.

As a final test of the validity of the correlation dimensions calculations, Haykin and Li randomize the phase of the Fourier spectrum from the original time clutter series to create a 'random' time series. The computed correlation coefficient for this 'random' series does not converge to a finite correlation dimension with increasing embedding dimension, instead the correlation dimension continues to expand to fill the available phase space, a behaviour consistent with a true random signal.

The third item, the existence of a positive Lyapunov exponent, is another necessary condition for a chaotic system. Using an algorithm developed by Wolf et al. [21] to estimate the largest Lyapunov exponent from a data set, Haykin and Li calculate the value corresponding to each set. They perform the calculation for the I-channel, Q-channel and amplitude data and report essentially identical results for each channel, a result anticipated from Taken's embedding theorem, which imposes no restrictions on the choice of the measured component used to reconstruct the attractor. As with the correlation coefficient they compare the variation of the calculated maximum Lyapunov component for different sea states and locations. While the calculated maximum Lyapunov exponent varies within a range of 0.03 to 0.04 they are unable to identify a clear relationship between the either the location or sea state and the calculated Lyapunov coefficients.

The final aspect to be considered by Haykin and Li was the issue of predictability. As with the earlier papers by Leung and Lo [13] and Leung [15] a neural network is constructed to model the non-linear dynamics of the underlying sea clutter model. For this study Haykin and Li utilize an MLP structure trained using the back propagation method, the details of the structure are not given here, the interested reader is referred back to the Haykin and Li paper. The development of the mapping neural network serves two purposes:

1) After training, the network can be used in a recursive (iterative) prediction mode to test the ability of the network to successfully predict the future behaviour of a real chaotic time series. This item relates back to the requirement of a chaotic system to

be deterministic (by definition), i.e. if we can successfully predict future behaviour of a real system then it is by nature deterministic.

2) The fully trained neural net can be used to detect targets in the measured chaotic time series. This is done in identical fashion to method described in the Leung and Lo [13], where the prediction error at each step is compared to specified threshold to determine whether a target is present or not.

Recursive (iterative) prediction uses new input samples from outside the original training set to initiate the prediction mode, each new predicted point is used to replace one of the components of the embedded time series in sliding window fashion until, eventually, the predictor begins to operate in autonomous fashion. Given the sensitivity of a chaotic system to its initial conditions it is not anticipated that the neural net predictor can correctly predict new values indefinitely, rather the local prediction time, T, should be inversely proportional to the largest Lyapunov coefficient as given by Farmer and Sidorowich [22],

$$T \approx \frac{1}{\lambda_1} \ln\left(\frac{\sigma_T}{\sigma_0}\right), \qquad (25)$$

where σ_0 is the uncertainty of the measurement at time T=0 and σ_T is the normalized standard deviation of the prediction error at time T into the prediction process. Haykin and Li report good agreement for the one example they present for which the calculated local prediction time is $T \approx 56$ while the observed local prediction time derived by comparing the recursively predicted values with the real measured values in the time series gives $T \approx 65$.

As a further check of the local prediction accuracy of the trained neural net predictor they average 100 different segments of 1024 samples from the predicted time series and the real measured time series. They then calculate the power spectrum of each. Good agreement is observed between the two sets. The same 100 segments of 1024 samples are used to plot the probability density of the predicted time series. The resulting distribution is shown to be in good agreement with a specially chosen theoretical K-distribution, the point being to show that the output from chaotic deterministic system is capable of exhibiting characteristics typically associated with random systems. This is an important point since any chaotic model of sea clutter must be compatible with previous observations that high-resolution sea clutter returns appear to well modelled by the K distribution.

Based on the analysis summarised above and their definition of a chaotic process, Haykin and Li assert that sea clutter is a chaotic process. They summarise their results as follows:

1) Sea clutter is bounded.

2) Sea clutter has a finite correlation dimension in the range of 7 to 9.

3) The largest Lyapunov exponent of sea clutter is positive and lies in the range 0.03 to 0.045. The value has a strong dependence on sea state.

4) Sea clutter is locally predictable and most importantly, the dynamics of sea clutter can be reconstructed using a deterministic model.

Haykin and Li next examined the ability to successfully use a neural predictor as a detector. Using the same neural detector design developed for the recursive prediction studies, Haykin and Li tested the detection capabilities of the chaos based system against a small ice target in a sea clutter background. They present ROC curves comparing the detection performance of chaos-based noncoherent detector against that of a conventional Doppler CFAR detector. The two methods produce similar results in their study despite the fact that the phase information is not used for the incoherent chaos detection. This was anticipated as a result of the embedding theorem.

They also present ROC curves comparing a coherent chaos detector and a conventional Doppler CFAR detector. The coherent chaos detector differs from the incoherent detector in that it performs separate predictions on the I and Q channels of the measured complex data, the prediction error of each channel is independently evaluated and the two 'channels' of prediction error are then subjected to conventional Doppler CFAR processing. Their results suggest that coherent chaotic detection will result in a 10-25% improvement in detection performance with respect to standard Doppler CFAR processing for the range of false alarms examined. Unlike Leung's earlier paper in which results were only presented for false alarm rates much too large for practical implementation, Haykin and Lo's results are presented for a range of false alarm probabilities from 10^{-1} to 10^{-5}. However the analysis assumes that long data sets are available, indeed 150 time samples are used to form each chaotic prediction and 256 samples are used for the Fast Fourier transform (FFT) length in the Doppler analysis. This condition if unlikely to be satisfied for any airborne maritime surveillance radar.

Haykin and Li's analysis is extensive and useful in establishing that many of the necessary conditions for the existence of a radar sea clutter attractor are present. Unfortunately while all these conditions are necessary they are not sufficient to prove the existence of the chaotic attractor.

A smattering of additional papers between the time frame 1995 through 1997 look at the issue of chaotic sea clutter. Palmer et al. [23] generate the correlation coefficient from several time series of X-band Doppler radar sea clutter returns collected with a coherent radar located 573 m above the sea surface on San Clemente Island. They observe convergence for the calculation of the correlation coefficient for the vertically polarized (VV) returns but not the horizontally polarized (HH) returns. They build a back-propagation neural network to predict the surface winds using the VV returns and report an improvement in the prediction accuracy over that of the SEASAT statistical algorithm. No explanation is given for the different convergence characteristics of the VV and HH returns.

Chakravarthi [24] examines the detection performance of a chaotic detector using simulated data from a known chaotic system. The time series output of this system has quantitative similarities to real sea clutter returns. As asserted previously by Haykin and Lo, the exploitation of the known chaotic properties of the systems allows the detection of the desired target in signals with very low signal to clutter ratios.

Haykin and Puthusserypady [25] expand on the previous analyses of Haykin and Li [16] by analysing five sea clutter sets collected from three different maritime locations using the fully coherent IPIX radar and another non-coherent commercial marine radar. They identify five criteria they claim are essential for evaluating whether a physical time series is chaotic:

1) The process should be non-linear.

2) The attractor (correlation dimension) should be fractal and should converge to a constant value for increasing embedding dimension.

3) The dynamics of the system responsible for the generation of the process should be sensitive to initial conditions. This in turn implies that at least one Lyapunov exponent should be positive.

4) The sum of all Lyapunov exponents of the process should be negative for the underlying dynamics to be dissipative (i.e. physically realizable).

5) The Kaplan-Yorke dimension (D_{KY}) should be close in numerical value to the correlation dimension. The relationship between the correlation dimension and the independently calculated D_{KY} provides a useful crosscheck of the correlation dimension [25].

As a prerequisite to any analysis, the embedding dimension, d_E, and normalized embedding delay, τ, must be calculated. In this study these parameters were obtained using the Global False Nearest Neighbours (GFNN) and Mutual Information (MI) algorithms, respectively. To determine the local embedding dimension, d_L, a Local False Nearest Neighbours (LFFN) algorithm was used. This value should correspond to the true number of Lyapunov exponents and should meet the criteria $d_L \leq d_E$.

The five criteria can now be addressed. To test the non-linearity of the time series, Haykin and Puthusserpady perform three separate tests.

In the first test they compare the original time series with the output of a finite impulse response filter that has been stimulated with zero-mean white Guassian noise. The spectral response of the filter is chosen to produce an output power spectrum identical to the original clutter time series. The two data sets (i.e. measured clutter returns and filtered noise signal) are compared with surrogate data sets created using a stochastic linear model with the same autocorrelation coefficients as the original time series. A quantity Z is derived from the Mann-Whitney rank-sum statistic; the value of this quantity is indicative of whether the original and surrogate data sets came from the same population [26]. For the filtered noise signal, the value of Z is always positive indicating that it is a linear process. The Z value for the actual sea clutter data is always less than –3.0 indicating that it is not from the same population as the stochastic linear model.

As a further comparison of the real and filtered noise signal, the correlation dimension, Lyapunov spectrum and the Kaplan-Yorke dimension are calculated for each set. To calculate the correlation dimension, Haykin and Puthusserpady utilise the maximum likelihood method

developed by Schouten et al. [27]. This method is chosen due to its superior noise performance over that of the Grassberger and Procaccia algorithm used in earlier reports [7]. As in the earlier study by Haykin and Li, the sea clutter data is filtered to improve the analysis. Haykin and Puthusserpady are careful to examine the diffeomorphic relationship of the filtered and unfiltered sea clutter by testing the continuity between the sets and as well as the differentiability of the mapping. They assert that their testing confirms the diffeomorphism of the two sets (i.e. the underlying dynamics of the sea clutter) are unaffected by the processing. Unlike Haykin and Li who calculated only the largest Lyapunov exponent, this study uses the algorithm of Brown, Bryant and Abarbanel [28, 29] to calculate the entire Lyapunov spectrum. In addition to providing the full spectrum this algorithm is claimed to be more stable in the presence of noise than Wolf's algorithm [21].

In summary the following results are reported for the clutter data and filtered noise signal (coloured noise) output from the finite impulse response filter:

1) The correlation value of the real sea clutter is fractal and saturates in the range of 4.1 through 4.5 for increasing embedding dimension while the value for the coloured noise keeps increasing with increasing embedding dimension.

2) The Lyapunov spectrum of the real sea clutter time series consists of two positive exponents followed by one exponent close to zero and two or more negative exponents. The sum of the exponents is always less than zero indicating a dissipative system. The Lyapunov spectrum of the coloured noise consists of several positive exponents and keeps increasing for increasing values of d_E. The sum of the exponents for $d_E < 7$ was always positive and non-dissipative.

3) D_{KY} and D_c are always very close for real sea clutter while for the coloured noise the two parameters are never close.

For the third and final test, the FFT of the real clutter time series is taken and surrogate data sets formed from the result by randomizing the phase of each frequency component. The correlation dimensions are computed for both the real and surrogate data sets and are statistically compared using a Student's t test. The surrogate data sets are found to be substantially different from the real sets.

All three of the above tests help to confirm the non-linearity of the sea clutter data. In summary Haykin and Puthusserypady report:

1) The correlation dimension is fractal and lies in the range 4.1 to 4.5. Its value is independent of the time or season in which it is taken, as well as radar range, range resolution, type of like-polarisation, sea state, radar location and radar type. It is also independent of the radar component used e.g. in-phase, quadrature-phase and amplitude component.

2) The global embedding dimension, d_E, is 5 or 6.

3) The local embedding dimension, d_L, (also corresponds to the number of Lyapunov exponents) is either 5 or 6 with $d_L \leq d_E$.

4) The Lyapunov spectrum consists of two positive exponents, followed by one exponent equal to zero (within experimental error) and two or three negative exponents. The distribution of the exponents is independent of radar range, radar component and sea state, although the absolute values of the exponents do depend on sea state and radar type.

5) The Kaplan-Yorke dimension, a by-product of the Lyapunov spectrum, is consistently close to D_c.

In 1999, Haykin again discusses the results of the Haykin and Puthusserypady and performs an independent calculation of the Kolmogorov entropy, h_K, using an algorithm based on the method of maximum likelihood. The introduction of this measure provides a useful cross check of the calculation of the Lyapunov spectrum as the two are related by the formula [27]

$$h_K = \sum_{\lambda_i > 0} \lambda_i . \quad (26)$$

Haykin reports that in all cases the relationship holds within a reasonable measurement error.

Haykin also confirms that the minimum data set size relationship of Eckmann and Ruelle [20] is met, namely a time series of length $N=10^{0.5Dc}$ is required to estimate the correlation dimension while the square of N is required to successfully estimate the Lyapunov exponents. For the maximum reported correlation dimension of 4.5, the required sample size is 31623, well below the 50,000 sample sets used by Haykin and Puthusserypady.

Most recently Lampropoulos and Leung [30] compared the CFAR detection performance of chaotic and statistical CFAR detectors. They use real sea clutter data derived from a SAR image and report an approximate 2 dB detection gain, however it is not clear what configuration they are employing for the statistical CFAR detectors and if they could be optimized for improved performance. The study is interesting but very limited.

Despite the foregoing investigations several key questions remain regarding the applicability of chaotic theory to sea clutter modelling. In summary:

1) A broad range of correlation coefficients have been reported, values range from 3 to 9. Although Haykin and Puthusserypady eventually conclude that the correlation coefficient is invariant against sea state, location and a variety of other parameters, the extreme range of reported values raises serious questions as to the reliability of the algorithms employed. It remains unknown how robust these algorithms are when applied to noisy data. Indeed the wide variability would seem to preclude the ability to render any conclusions on the 'fractal' value of the correlation coefficient.

2) It remains unclear whether the invariant measures of 'chaotic' systems that were calculated could in fact merely represent the effect of non-chaotic deterministic

systems with additional coloured noise added to the system. The potential for linear dynamic systems with noise to produce positive Lyapunov exponents is recognized by Theiler et al [30].

3) The increases in detection performance are only reported for a limited sampling of data sets and, by implication, conditions. The applicability of the methods to a broad range of sea states, weather conditions and viewing geometries is currently unknown. Certainly the reported detection performance improvements of 2-3 dB are well below the anticipated improvements for truly chaotic systems. Whether the use of a non-linear chaotic detector instead of a simpler linear detector is justified remains an open question.

4) The clutter noise ratios required is unclear and could prove to be impractically high.

5) The studies examined have used relatively low resolution data with a range resolution of 30 m or more. The application of the method of to a typical airborne high bandwidth radar with a resolution of less than 1 metres is currently unknown.

Some of the key findings of the most relevant studies discussed above are listed in Table1.

Table 1. Summary of results from chaos studies.

Study	Length of Time Series	Correlation Dimension D_c	Sum of Lyapunov exponents < 0	Existence of at least one positive Lyapunov exponent
Leung and Haykin [5]	2000	6.4-6.7	Not Calculated	Not Calculated
Leung and Lo [13]	20,000	5.8-7.2	Not Calculated	Not Calculated
Blacknell and Oliver [14]	2,000	3-4	Not Calculated	Not Calculated
Haykin and Li [16]	40,000	7-9	Not Calculated	Yes
Haykin and Puthusserpady [25]	40,000	4.1-4.5	Yes	Yes

6. Chaotic Behaviour of Sea Clutter from an Airborne Radar

Almost all the studies summarized in the proceedings sections were based on analysis of sea clutter collected using land based radars operated in staring modes at grazing angles of less than 1°. This is a significant limitation as one of the most important potential applications of chaos based protectors is their application to the small target detection from airborne radars.

The specification of an airborne platform has a number of implications. Typically these systems are large bandwidth radars operating at range resolution of less than metre; most of the previous studies reviewed in this report relied on data collected with land based radar's having range resolutions of 30m or greater. The geometry of the airborne viewing scenario also results in steeper grazing angles then those obtained with a land based system. The grazing angles encountered in the airborne data examined in this report range from 1.8° to 9°. Another important distinction with an airborne system is that the radar platform is moving. It has been speculated that this movement would merely represent an additional degree of freedom in an already deterministic systems [16] but until now the effect has remained unexamined. Indeed, it is possible that the existence of non-stationarity with location of the underlying attractor could prevent the development of real time chaotic detectors.

To better understand these effects a study was undertaken by DREO in cooperation with Dr. Leung's group at the University of Calgary to examine high resolution sea clutter data collected from an airborne platform with the AN/APS-506 radar. The investigation is structured along similar lines to the investigation of Haykin and Puthusserypady with the hope that the similarities and differences of the land based low resolution and airborne high resolution measurements can be highlighted.

6.1 Airborne Data Set

The characteristics of the AN/APS-506 maritime radar are summarized in Table 2 below. All files analyzed are summarized in Table 3 along with the operational configuration that was employed during the collection process. The viewing direction with respect to the sea swell is also noted where applicable. Each time series was constructed from temporally contiguous measurements of returns from the same range bin, i.e. a measurement was taken from the same range bin for each pulse return. Each sample will therefore correspond to the return from a different geographic location on the sea surface. The manner in which the returns migrate across the sea surface will depend on the operating mode described in Table 3, e.g. squint, rotating or sectoring. Sea state was not recorded.

Table 2. *Operating parameter of AN/APS-506 maritime radar.*

PARAMETER DESCRIPTION	PARAMETER VALUE
Frequency	9.5-10 GHz
Peak Power	500 kW
Azimuth Beamwidth	2.4°
Elevation Beamwidth	4°
Polarization	Horizontal-Horizontal
Sidelobes	-20 dB

6.2 Preconditioning of Airborne Data

Before analysis the data was preconditioned to minimize the effect of measurement noise on the analysis. A simple smoothing filter of the form

$$\hat{y}(n)=\sum_{i=1}^{3}\frac{1}{3}y(n+i-2) \qquad (27)$$

was applied as per the approach of Haykin and Puthusserypady [25]. To support the assertion that the filtered and unfiltered data trajectories are diffeomorphically related, the continuity and differentiability of the mapping between the two time series was tested. The continuity and differentiability index were calculated as per the approach of Haykin and Puthusserypady using an embedding dimension of 7 (independently determined to be the appropriate embedding dimension as discussed below). Figure 8 presents a plot of the continuity index versus epsilon for five different data sets where epsilon is the fraction of the variance for the particular time series. It can be seen that for all data sets the continuity index converges to one as the epsilon value is increased to a sufficiently large value to allow a statistically meaningful sampling of data points. For all files examined in the data set the continuity index ranges between 0.82 and 1.0.

Figure 9 shows the differentiability index versus epsilon for the same five data sets, the value converges to approximately one for all five sets.

Table 3. *Operational configuration of radar during collection of clutter data files*

FILE NAME	PRF (HZ)	ANTENNA DEPRESSION ANGLE (^{O})	VIEWING ANGLE	RESOLUTION	OPERATNG MODE
HDR472s14	672	2.39	Down-swell	<1m	Squint 85 Degrees
HDR472s15	672	2.39	"	<1m	"
HDR472s16	685	4.54	"	<1m	"
HDR472s17	692	8.97	"	<1m	"
HDR472s19	715	8.93	Cross-swell	<1m	"
HDR472s20	711	4.56	"	<1m	"
HDR472s21	711	2.40	"	<1m	"
HDR472s95	314	5.59	N/A	5m	Rotating @ 1 RPM
HDR472s96	314	5.59	N/A	5m	"
HDR473s58	172	1.81	N/A	5m	Rotating @1 rpm
HDR473s59	172	1.81	N/A	5m	"
HDR473s60	172	1.81	N/A	5m	"
HDR473s61	172	1.81	N/A	5m	"
HDR473s62	172	1.81	N/A	5m	"
HDR475s29	353	3.41	N/A	5m	Rotating @ 0.5 rpm
HDR475s30	353	3.41	N/A	5m	"
HDR475s31	353	3.41	N/A	5m	"
HDR475s32	353	3.41	N/A	5m	"
HDR475s33	353	3.41	N/A	5m	"
HDR475s34	353	3.41	N/A	5m	"
HDR475s35	353	3.41	N/A	5m	"
HDR475s36	353	3.41	N/A	5m	"
HDR475s37	353	3.41	N/A	5m	"
HDR418s39	590	5.84	N/A	<1m	Sectoring over 20 degrees at effective speed of 6 rpm
HDR418s40	590	5.84	N/A	<1m	"

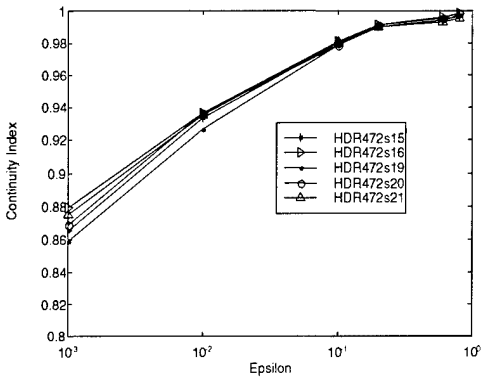

Figure 8. *Continuity index versus epsilon for selected data sets and embedding dimension of 7.*

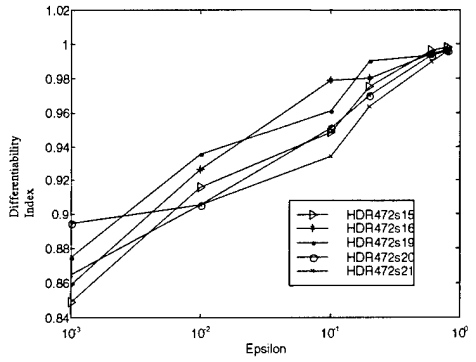

Figure 9. *Differentiability index versus epsilon for selected data sets and embedding dimension of 7.*

6.3 Time Delay and Embedding Dimension Estimation for Airborne Data

The appropriate time delay was calculated using the first minimum of the mutual information function. When the time delay was calculated using the unfiltered data many of the data files

produced a minimum at a delay of one. This is illustrated in figure 10 for the plot of the mutual information function versus delay for one unfiltered time series.

Since a delay of one represents the fundamental minimum resolution that can be derived from the given time series it is unclear if it is in fact an optimum delay or if the measured samples were so widely spaced they have completed de-correlated over the sampling interval. The calculation was repeated on the filtered data and the optimum delay was found to vary between 5 and 20 indicating that the delay of one was a result of de-correlation due to measurement noise. Figure 11 shows an example the plot of the mutual information function versus delay for a filtered time series where an approximate optimum delay of 20 is indicated. It is unclear why the optimum delay varies over so broad a range although sea state or atmospheric conditions may have an effect through their impact on the Lyapunov exponents discussed later in this report.

The embedding dimension was next calculated using the method of false nearest neighbours [32]. A sample FNN plot of the filtered time series versus embedded dimension is shown in figure 12. In this example the percentage of FNN never falls below 40%. Figure 13 illustrates another time series in which the FNN more closely approaches the zero limit.

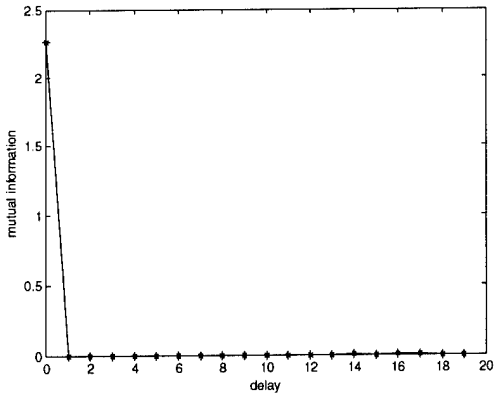

Figure 10. *Mutual information versus delay for unfiltered time series HDR472s14, range bin 361.*

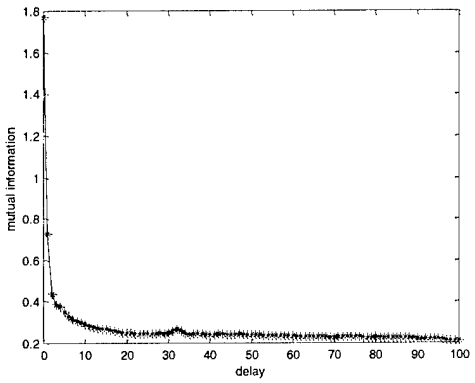

Figure 11. *Mutual information versus delay for filtered time series HDR473s58, range bin 361.*

Figure 14 and 15 display histograms of the calculated embedding delays and embedding dimension respectively. The broad range of calculated embedding delays is clearly seen in figure 14 while the measured embedding dimensions are tightly concentrated in the range of 6 to 7. As discussed above, Haykin and Puthusserypady [25] report an embedding dimension of 5 to 6. While it might be speculated that the increased embedding dimensions arise as a result of the additional degree of freedom introduced by the moving platform of the airborne system, the reason for this difference remains unclear.

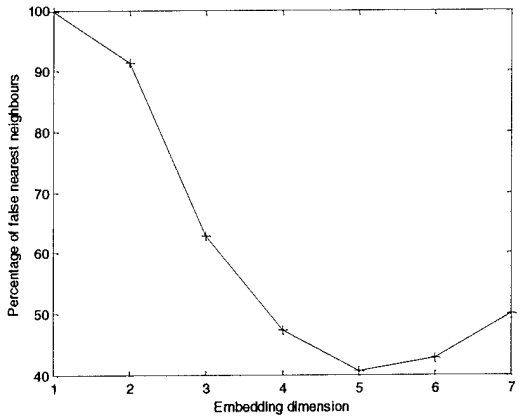

Figure 12. *Percentage of FNN versus embedding dimension for data set HDR472s15.*

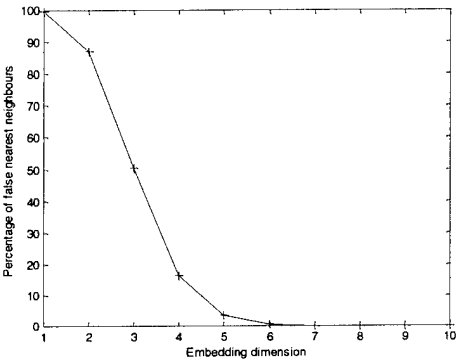

Figure 13. *Percentage of FNN versus embedding dimension for data set HDR472s95.*

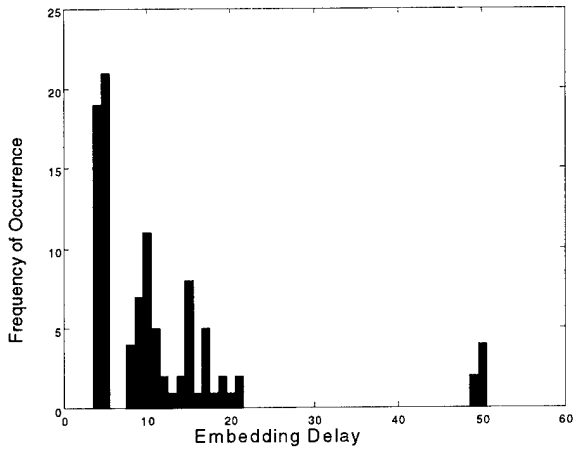

Figure 14. *Histogram of embedding delays calculated from all data sets.*

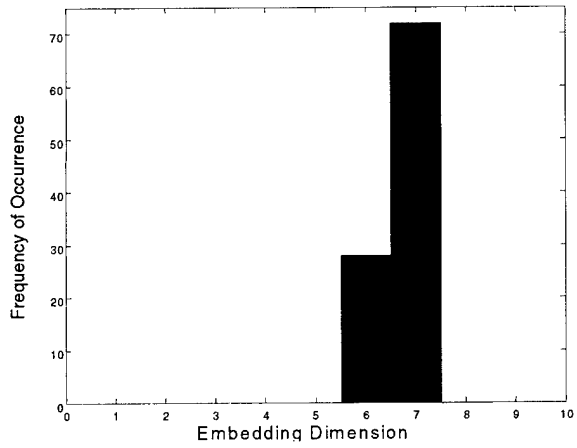

Figure 15. *Histogram of embedding dimensions calculated from all data sets.*

6.4 Analyses of Airborne Data

With the embedding delay and embedding dimension determined as discussed above, the airborne data was then analyzed to determine the following parameters:

1) Correlation dimension

2) Lyapunov exponents and Lyapunov dimension

6.4.1 Correlation Dimension of Airborne Data

The correlation dimension was calculated using two independent methods. The first method utilizes a least squares (LS) fitting as outlined in section 3.1 for equation (9). Because of the LS method's sensitivity to noise the correlation dimension has also been derived using the maximum likelihood (ML) approach of Schouten et al. [7]. Figure 16 presents the histogram of results calculated using each approach on filtered data. The results from both approaches show good agreement. Figure 17 presents the histogram of results produced using the ML approach on filtered and unfiltered data.

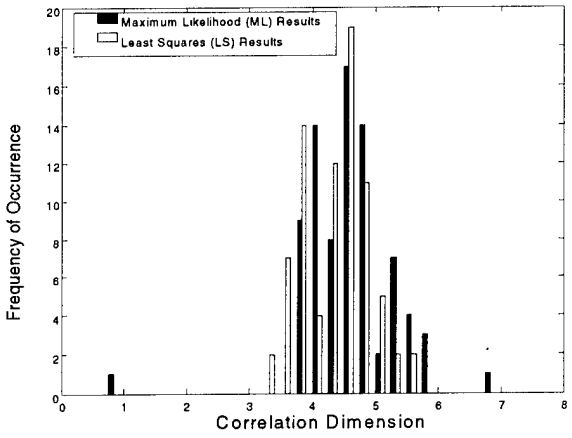

Figure 16. *Histograms of correlation dimensions calculated from all filtered data sets using LS and ML techniques.*

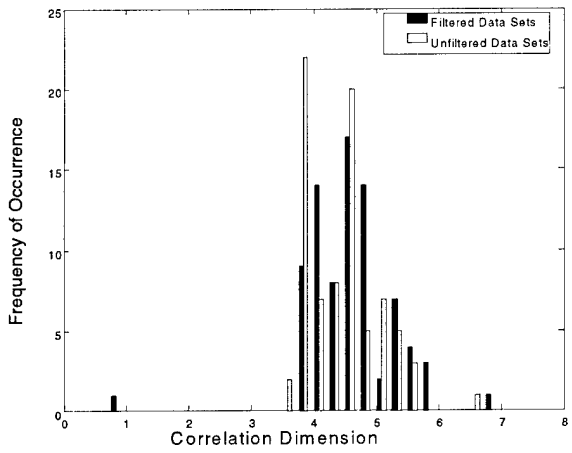

Figure 17. *Histograms of correlation dimension calculated from filtered and unfiltered data sets using ML technique.*

The average measured correlation value calculated from the filtered data is 4.42 and 4.63 for the LS and ML techniques respectively. The average measured correlation value calculated from the filtered data and unfiltered data is 4.63 and 4.49, respectively. The range of measured correlation values is consistent with those measured by Haykin and Puthusserypady [25] who reported a range of 4.1 to 4.5.

This level of consistency is remarkable when one considers that:

a) the measurements analyzed in this report were taken with a radar on a moving airborne platform without any attempt to compensate for motion
b) the data set is composed of very high range resolution measurements of less then a meter.

Perhaps most intriguing is the stability of correlation dimension with resolution. The data of Haykin and Puthusserypady was derived from 30-300 m resolution data; 'low resolution' measurements such as these typically display a Guassian-like distribution when their probability distribution is plotted. In contrast the sub-metre high resolution measurements used in this study have a probability distribution plot well modeled by the K-distribution. The character of the two distributions (Guassian and K-distribution) can be quite different and it is unclear how these differences should be reflected in the calculated chaotic invariants. Further studies are required to investigate the relationship, possibly diffeomorphic, between the high resolution and low resolution returns and to establish if the consistency is indeed a real property of sea clutter returns or merely a limitation of the algorithms used to calculate it.

6.4.2 Lyapunov Exponents and Lyapunov Dimension of Airborne Data

The Darbyshire and Broomhead [33] technique, hereafter referred to as the DB technique, is used to calculate the Lyapunov spectrum. This method is chosen due its enhanced stability in the presence of noise in comparison with earlier techniques. Figure 18 displays a typical spectrum calculated from one data set.

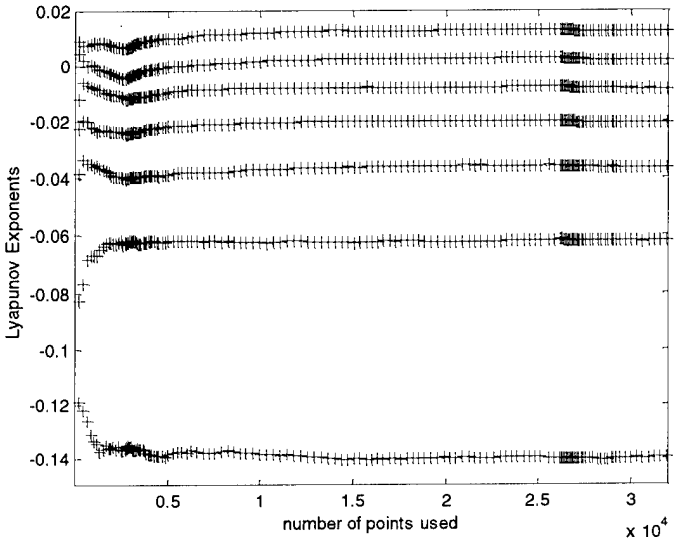

Figure 18. *Lyapunov spectrum calculated for data set HDR472s95, range bin 600.*

Three general features, consistent with real life chaotic behaviour, are observed in the calculations for all data sets:

1) All spectrums contain at least one Lyapunov exponent that is very close to zero. As discussed in section 3.2, this a fundamental property of any bounded attractor of an autonomous system.

2) The sum of Lyapunov exponents in each spectrum is less than zero, this is indicative of an underlying process that is dissipative in nature (typical of real world dynamical systems).

3) Each spectrum contains at least one positive Lyapunov exponent, a necessary requirement if a system is to display chaotic behaviour.

Figure 19 displays a histogram of the largest Lyapunov exponent from each data set. As observed in other studies the largest exponent can be distributed over a range of values and Haykin and Puthusserypady observed a positive correlation of with sea state. Unfortunately sea

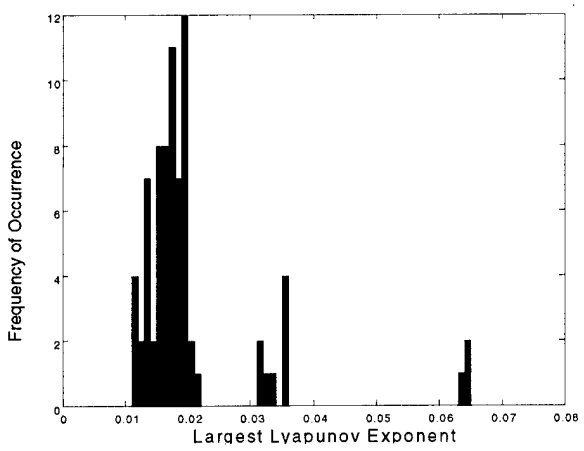

Figure 19. *Histogram of largest Lyapunov values from each data set.*

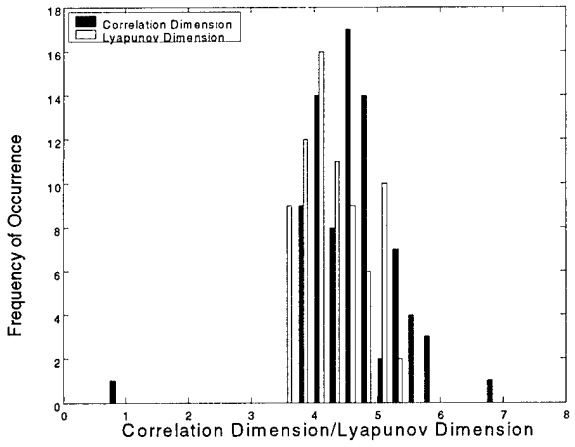

Figure 20. *Histogram of Lyapunov dimensions from all data sets.*

state values are not available for the data set used in this study and any connection between increased sea state and increased maximum Lyapunov exponent cannot be verified.

As discussed in section 3.2, the calculation of the Lyapunov dimension provides a useful crosscheck of the correlation dimension as the two parameters should be close in value, although not necessarily equal. Figure 20 presents a histogram of the Lyapunov dimensions

from all data sets and the correlation dimension calculated from the filtered data using the ML technique.

6.4.3 Non-linearity of Airborne Data Sets

Two tests were performed to lend confidence to the statement that data sets under consideration are indeed generated by a nonlinear dynamic system. The tests compare the actual data sets with surrogate data sets from linear stochastic processes. The two tests are as follows

1) Correlation coefficient of randomized data (RD) sets – In this test the fast Fourier transform (FFT) of data set is taken and the phase components of the resulting spectrum randomized by choosing the phases from a set of uniformly distributed values between 0 and 2π generated using a random number generator. The resulting spectrum is then inverse FFTed to produce a surrogate data set with the same autocorrelation function as the initial real time series. The act of randomizing the phases causes the surrogate data sets to become more Guassian in character. The correlation dimension of the resulting surrogate data set is computed and compared with the original data set.

2) Statistical comparison of stochastic linear (SL) data with sea clutter data – The growth of the inter-point distances is measured between the real sea clutter data and surrogate data sets generated from a stochastic Guassian linear model with the same autocorrelation coefficients. A quantity, Z, is calculated from the Mann-Whitney rank-sum statistic. A value of less than –3.0 is considered sufficient to rule out the null hypothesis that the surrogate and real data sets are drawn from the same stochastic model.

Figure 21 displays the histograms of the correlation coefficients calculated using the ML technique on the originals data sets and the RD sets using an embedding dimension of 7. The RD data sets produce a higher calculated correlation dimension with an average value of 8.45. Another significant difference is that the calculated correlation dimension of the surrogate data sets keeps increasing as the embedding dimension is increased beyond the value of 6 earlier determined using the FNN approach. This expansion of the correlation dimension to fill the available phase space is typical of a noise process. This is illustrated in figure 22 for one data set.

The significant differences in correlation coefficients between real data and surrogate data sets strongly suggest the sets are drawn from unrelated populations. However, the test does not definitively prove that the real data sets are non-linear but merely confirms that the surrogate data sets, which are essentially linear Guassian processes, are fundamentally different from the real data sets.

The results of the second test are displayed in figure 23 as a histogram of the calculated Z values from all the data sets. It is readily evident that the calculated Z values are less than negative 3.0 for most of the data sets examined. Once again it can be concluded that the real data sets are not represented by a Guassian linear model.

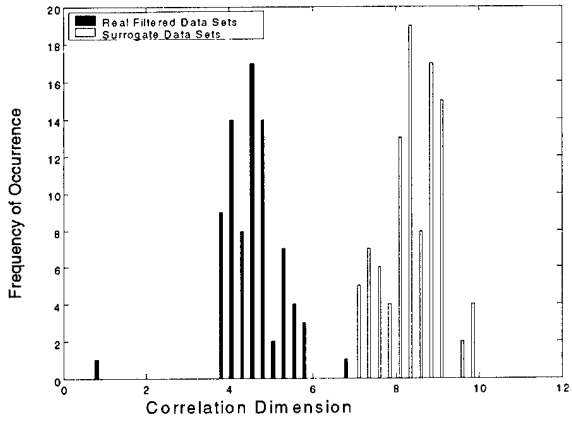

Figure 21. *Histogram of correlation dimensions calculated from real data sets and surrogate RD data sets.*

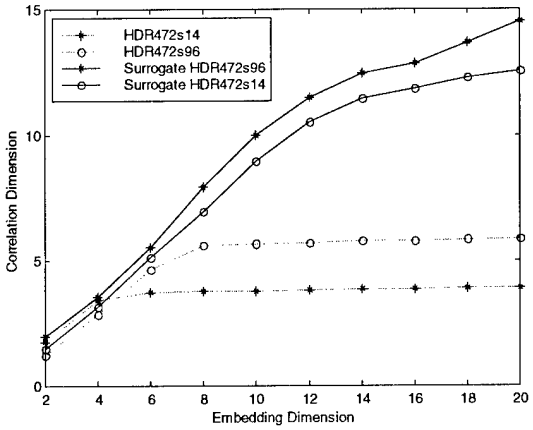

Figure 22. *Plot of calculated correlation dimension versus embedding dimension for RD surrogate data sets and real data sets HDR472s14 and HDR472s96..*

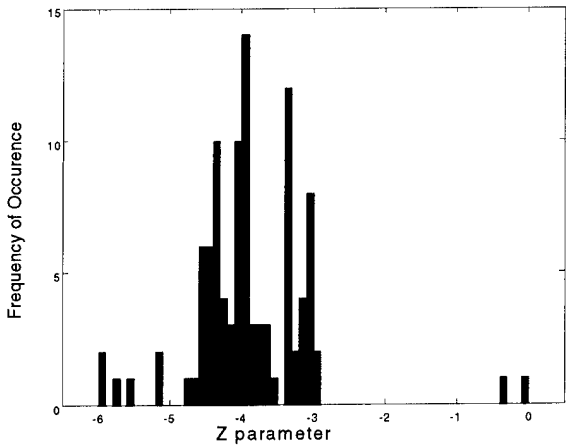

Figure 23. *Histogram of Z parameter calculated from comparison of real data sets and surrogate SL data sets.*

6.5 Prediction Performance for Airborne Data

The ultimate goal of applying chaotic theory to the sea clutter problem is exploit its deterministic nature so as to develop accurate predictors for sea clutter returns. As discussed in section 3, this ability to accurately predict sea clutter returns via a non-linear chaotic model should in theory, produce substantial improvements in detection performance over that of stochastic models. In the following sections the performance of two different predictors is examined and as a necessary precursor to the development of a predictor the stationarity of the data sets is examined. Clearly the development of any real predictor scheme for use in real radar detections is dependent on the underlying attractor structure remaining stationary between the time the predictor is trained and the latest prediction is attempted.

6.5.1 Stationarity of Airborne Data Sets

Figure 24 is an example of a recurrence plot for one of the real data sets. The fairly uniform nature of the plot confirms the stationarity of the time series [34]. Other data sets produce similar results.

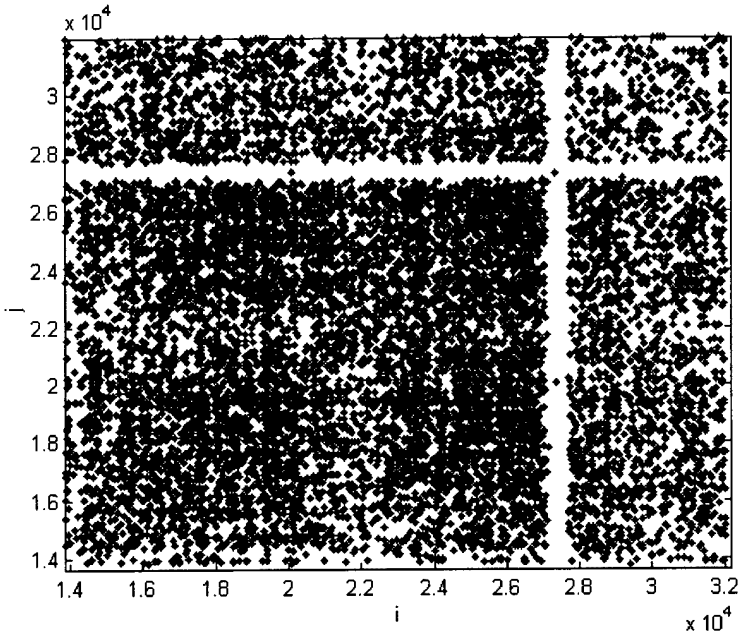

Figure 24. *Recurrence plot for data set HDR472s14, range bin 361, embedding dimension 7, r=45% of standard deviation.*

6.5.2 Prediction Analysis for Airborne Data

Two different approaches are used to construct the predictor, a local linear technique and a radial basis function.

The local linear technique works by developing a look up table of values during its training. After training, the neighbours of the current point are fitted to a linear function to produce a prediction. In the simple zeroth order predictor used in this study the prediction is formed using a simple average of the state space neighbours surrounding the current point.

The radial basis function technique is a global interpolation technique with good localization properties. The form of the predictor used in this study is given as

$$F(\mathbf{x}) = \sum_{j=1}^{n_c} \lambda_j \phi(\| \mathbf{x} - \mathbf{c}_j \|) \qquad (28)$$

where $\phi(r) = e^{\frac{-r^2}{\sigma^2}}$ is constructed about n_c number centres (c_j), with the constant σ being determined as a multiple of the average distance between data points considered in the fit. The λ_j constants are determined by a least squares fit to the observations in the learning set,

$$b = A\lambda \qquad (29)$$

where b are the observations, λ is a vector of length n_c whose jth component is λ_j and A is given by

$$A_{ij} = \phi(\|x_i - c_j\|) \qquad (30)$$

The number of centres as well as the multiple of the average distances between the data points is fixed [12].

Figures 25 and 26 show two examples of predictions performed using the zeroth order predictor and radial basis function. The actual and predicated time series are shown above and the mean square error (MSE) between them, below. The actual real data series used for training and prediction was normalized to a range of +/- 1 for ease of comparison.

Each predictor was trained with a data set of 20000 points and then used to predict 200 steps forward in one step fashion i.e. the most recently acquired real measured values are used as the input for the next prediction step. No attempt is made to predict further than one step beyond the most recently measured d_E values at any time. The zeroth order predictor was restricted to use a minimum of 4 neighbours and a maximum of 50 neighbours for each step. In the case of the radial basis function, the number of random centers was fixed at 150 and the variance of the radial basis functions was fixed at 0.001.

Figure 27 presents histograms of the average MSE measured from 50 range bins in 8 different data sets using the zeroth order predictor and the radial basis function. Both methods produce similar results with an average MSE of 0.00325 and 0.00319 across the data sets for the radial basis function and zeroth order predictor respectively.

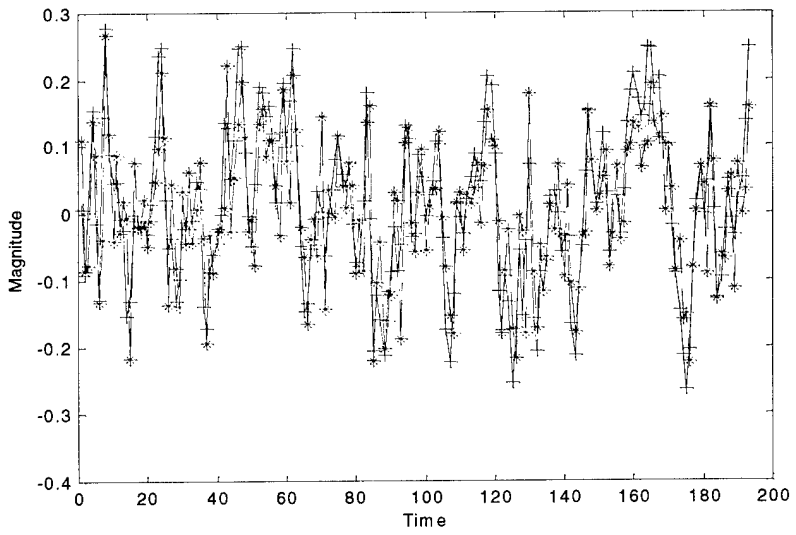

(a)

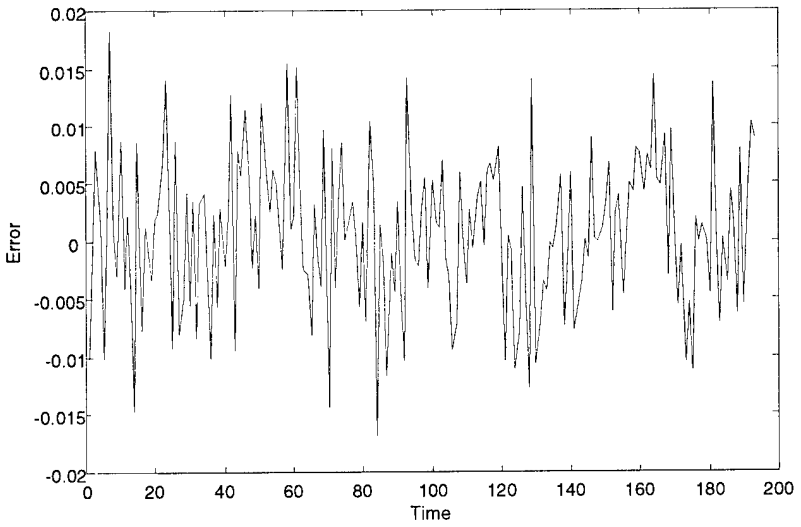

(b)

Figure 25. *Zeroth order prediction of time series HDR472s15 a) Times series of real data and predicted time series b) MSE between real time series and predicted time series.*

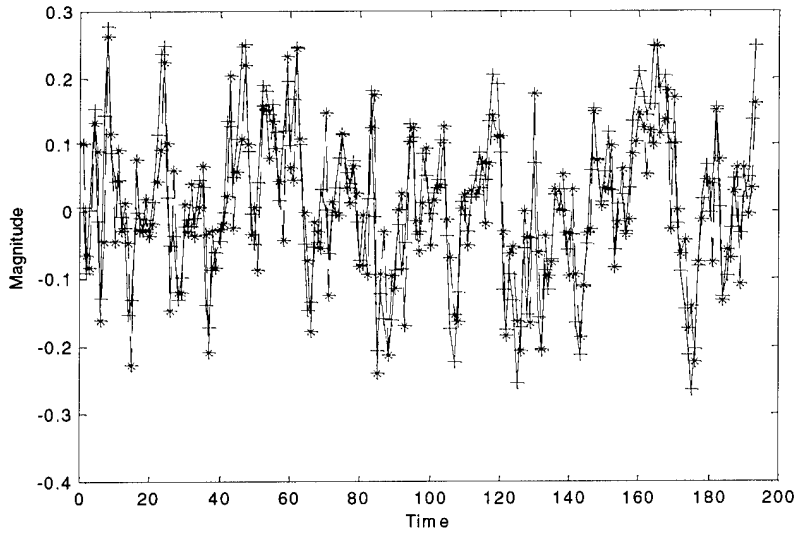

(a)

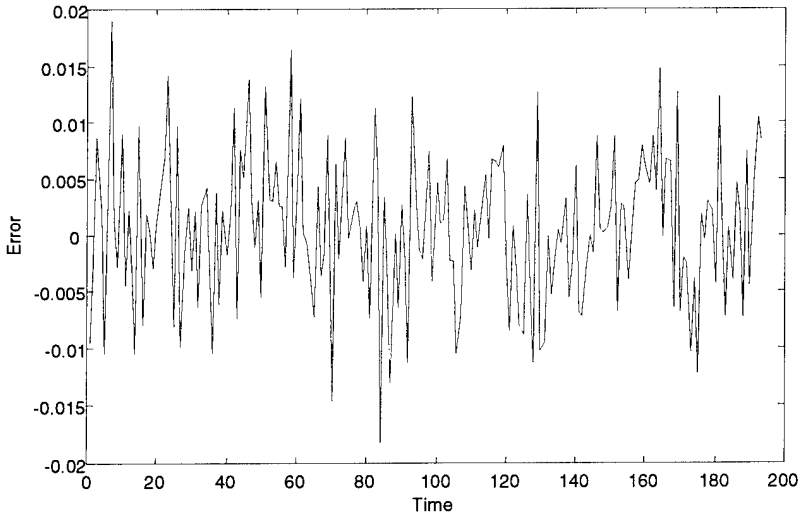

(b)

Figure 26. *Radial basis function prediction of time series HDR472s15 a) Times series of real data and predicted time series b) MSE between real time series and predicted time series.*

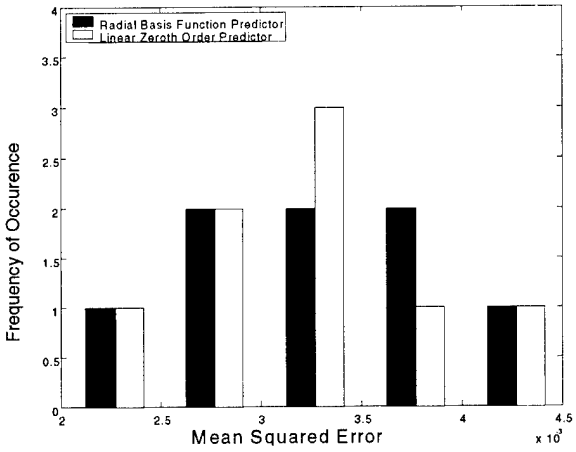

Figure 27. *Histogram of MSE between real time series and predicted times series in 50 range bins in each of 8 sets.*

7. Conclusions

Past studies, coupled with an evaluation of new high resolution airborne data suggest that chaotic dynamic systems may form an effective model of sea clutter returns. If a detector based on the predictive properties of chaotic systems can be developed it raises the possibility of dramatically improving detection performance over that of detectors based on stochastic approaches.

In this study several key parameters of chaotic dynamic systems, namely correlation dimension, Lyapunov spectrum and Lyapunov dimension were calculated using the high resolution sea clutter returns from the AN/APS-506 radar and found to be consistent with a chaotic interpretation of the dynamics. This study extends the results of Haykin and Puthusserypady which showed that the calculated correlation coefficients of real sea clutter were independent of the time or season in which it is taken, as well as radar range, range resolution, type of like-polarisation, sea state, radar location and radar type for two different low resolution radars operating in a fixed staring mode. In this report high resolution data (less than one metre) collected from a moving airborne platform produces a correlation coefficient with an average value of 4.63 and a standard deviation of 0.73, roughly consistent with the range of 4.1-4.5 reported by Haykin and Puthusserypady. However the airborne data differs in that it displays an embedding dimension of 6-7 in contrast with the 5 to 6 range reported by Haykin and Puthusserypady. A comparison of Lyapunov spectrums is not possible due to their dependence on sea state which was not recorded for the airborne data.

The airborne sea clutter data was compared with two different surrogate data sets composed of linear Guassian time series generated by randomizing the phase of the real data power spectrum and using a linear stochastic random number generator, respectively. Comparison of the correlation coefficients from the real data time series and the randomized phase sets shows substantially different correlation coefficients indicating that the two sets are dynamically unrelated. A statistical comparison of the real data set with time series generated using a random number generator for a stochastic Guassian model also indicates that the real data sets are not represented by this linear statistical model.

Despite the above evidence a number or fundamental questions remain unresolved.

1) A broad range of correlation coefficients has been reported over the past 10 years with values ranging from 3 to 9 [5,10,13,14,15,16,24,25]. The data examined in this report produces results consistent with those of Haykin and Puthusserypady who concluded that the correlation coefficient is invariant against sea state, location and a variety of other parameters. However, the extreme range of reported values raises serious questions as to the reliability of the algorithms employed [25]. It remains unknown how robust these algorithms are when applied to noisy data. Indeed the wide variability would seem to preclude the ability to render any conclusions on the 'fractal' value of the correlation coefficient.

2) The increases in detection performance are only reported for a limited sampling of data sets and, by implication, conditions. The applicability of the methods to a broad

range of sea states, weather conditions and viewing geometries is currently unknown. Certainly past reported detection performance improvements of 2-3 dB are well below the anticipated improvements for truly chaotic systems [13,15,16]. Whether the use of a non-linear chaotic detector instead of a simpler linear detector is justified remains an open question.

3) The clutter to noise ratios required for successful chaotic prediction remains unclear and could prove to be impractically high [14].

The deterministic character of the sea clutter returns is tested by developing a one step non-linear predictor. Two different approaches are implemented, a local linear technique and a radial basis function (RBF) neural network. A mean square error (MSE) of approximately 0.0032 is measured between the predicted and normalized real time series for both approaches. While a degree of predictability is demonstrated by this result it remains unclear whether the non-linear predictor will provide superior results in comparison to other more traditional detection schemes under real world detection scenarios.

The analysis in this report was confined to determining if the temporal variations in sea clutter returns collected from an airborne maritime radar were consistent with a chaotic interpretation. The results discussed provide qualified support for this interpretation. Future studies will examine the potential of exploiting the deterministic nature of chaotic processes to allow enhanced detection of targets in sea clutter. To clarify this issue, follow up studies will examine the detection performance of a non-linear detector and compare it against the performance achieved using more traditional methods such as CA-CFAR and stochastic coherent detectors.

References

[1] M. Skolnik, *Introduction to Radar Systems*, McGraw-Hill Book Company, Toronto, 1980.

[2] K.D. Ward, C.J. Baker and S. Watts, "Maritime surveillance radar Part 1: Radar scattering from the ocean surface," *IEE. Proc.*, vol. 137, Pt. F, no. 2, pp.51-62, 1990.

[3] S. Watts, C.J. Baker and K.D. Ward, "Maritime surveillance radar Part 2: Detection performance prediction in sea clutter," *IEE. Proc.*, vol. 137, Pt. F, no. 2, pp.63-72, 1990.

[4] K. J. Sangston, F. Gini, M.V. Greco and A. Farina, "Structures for Radar Detection in Compound Guassian Clutter," *IEEE Trans. on Aerospace and Electronic Systems*, vol. 35, no. 2, pp. 445-458, 1999.

[5] H. Leung and S. Haykin, "Is there a radar clutter attractor?," *Appl. Phys. Lett*, vol. 56, no. 6, pp. 593-595, 1990.

[6] T.S. Parker and L.O. Chua, "Chaos: A Tutorial for Engineers," *Proc. IEEE*, vol. 75, no. 8, pp. 982-1008, 1987.

[7] P. Grassberger and I. Procaccia, "Measuring the strangeness of strange attractors," *Physica 9D*, pp.189-208, 1983.

[8] H.Haken, "At least one Lyapunov exponent vanishes if the trajectory of an attractor does not contain a fixed point," *Phys. Lett.*, vol. 94A, no. 2, pp71-72, 1983

[9] P. Frederickson, J.L. Kaplan, E.D. Yorke and J.A. Yorke, "The Lyapunov dimensions of strange attractors," *J. Diff. Eq.*, vol. 49, pp. 185-207, 1983.

[10] S. Haykin, "Radar Clutter Attractor: implications for physics, signal processing and control," *IEE Proc.-Radar, Sonar, Navig.*, vol. 146, no. 4, 1999.

[11] F. Takens, "Detecting strange attractor in turbulence," in *Dynamical Systems and Turbulence*, Warwick 1980, D.A. Rand and L.S. Young Eds. Springer-Verlag, Lecture Notes in Mathematics, vol. 898, pp. 366-381, 1981.

[12] S. Haykin, *Neural Networks A Comprehensive Foundation*, Prentice-Hall, Upper Saddle River, 1999.

[13] H. Leung and T. Lo, "Chaotic Radar Signal Processing over the Sea," *IEEE J. Oceanic Engineering*, vol. 18, no. 3, pp. 287-295, 1993.

[14] D. Blacknell and C.J. Oliver, "Recognising chaos in radar images," *J. Phys. D: Appl. Phys.*, vol. 27, pp. 1608-1618, 1994.

[15] H. Leung, "Applying Chaos to Radar Detection in an Ocean Environment: An Experimental Study," *IEEE J. Oceanic Engineering*, vol. 20, no. 1, pp. 56-64, 1995.

[16] S. Haykin and X.B. Li, "Detection of Signals in Chaos," *Proc. IEEE*, vol. 83, no. 1, 1995.

[17] A.R. Osborne and A. Provenzale, "Finite correlation dimension for stochastic systems with power-law spectra," *Physica*, vol. D35, pp. 357-381, 1989.

[18] S. Newhouse, "Understanding chaotic dynamics," in *Chaos in Nonlinear Dynamical Systems*, J. Chandra, Ed. SIAM, 1984.

[19] F.J. Pineda and J.C. Sommerer, "A fast algorithm for estimating generalized dimensions and choosing time delays," in *Time Series Prediction: Forecasting the Future and Understanding the Past*, Addison-Wesley, Reading, MA, pp. 367-385, 1994.

[20] J.P. Eckmann and D. Ruelle, "Fundamental limitations for estimating dimensions and Lyapunov exponents in dynamical systems," *Physica*, vol. D56, pp. 185-187, 1992.

[21] A. Wolf, J.P. Swift, H.L. Swinnery and J.A. Vastano, "Determining Lyapunov exponents from a time series," *Physica*, vol. 16D, pp. 285-317, 1985.

[22] J.D. Farmer and J.J. Sidorwich, "Predicting chaotic time series," *Phys. Rev. Lett.*, vol. 59, no. 8, pp. 845-848, 1987.

[23] A. J. Palmer, R. A. Kropfi and C. W. Fairall, "Signatures of deterministic chaos in radar sea clutter and ocean surface winds," *Chaos*, vol.3, pp.613-616, 1995.

[24] P.Chakravarthi, "Radar target detection in chaotic clutter," *IEEE National Radar Conference*, pp.367-370, May 1997.

[25] S. Haykin and S. Puthusserypady, "Chaotic dynamics of sea clutter," *Chaos*, vol. 7, no. 4, pp. 777-802, 1997.

[26] S. Siegel, *Non-parametric Statistics for Behavioral Sciences*, McGraw-Hill, Japan, 1956.

[27] J.C. Schouten, F. Takens and C.M. Van den Bleek, "Estimation of dimension of a noisy attractor," *Phys. Rev. E*, vol. 50, pp.1851-1861, 1994.

[28] R.Brown, P. Bryant and H.D.I. Abarbanel, "Computing the Lyapunov exponents of dynamical systems from observed time series," *Phys. Rev. A*, vol. 43, pp. 2787-2806, 1991.

[29] P. Bryant, P. Bryant and H.D.I. Abarbanel, "Lyapunov exponents from observed time series," *Phys. Rev. Lett.*, vol. 65, pp. 1523-1526, 1990.

[30] G.A. Lampropoulos and H. Leung, "On CFAR detection of small man made targets using chaotic and statistical CFAR detectors," *SPIE Conf. Signal and Data Processing of Small Targets*, vol. 3809, pp. 29-41, 1999.

[31] J. Theiler, S. Eubank, A. Longtin, B. Galdrikian, and J. Farmer, "Testing for nonlinearity in time series: the method of surrogate data," *Physica D*, vol. 58, pp. 77-94, 1992.

[32] Matthew B. Kennel, Reggie Brown and Henry D.I. Abarbanel, "Determining Embedding Dimension for phase-space reconstruction using a geometrical construction," *Physical Review A*, vol. 45, pp. 3403, 1992.

[33] A.G.Darbyshire and D.S.Broomhead, "Robust Estimation of Tangent Maps and Liapunov Spectra," *Physica D*, vol. 89, pp.287-305, 1996.

[34] J.P.Eckmann, S.Oliffson Kamphorst and D.Ruelle, "Recurrence Plots of Dynamical Systems," *Europhysics Letters*, vol. 4, pp.973-977, 1987.

DOCUMENT CONTROL DATA

(Security classification of title, body of abstract and indexing annotation must be entered when the overall document is classified)

1. ORIGINATOR (the name and address of the organization preparing the document. Organizations for whom the document was prepared, e.g. Establishment sponsoring a contractor's report, or tasking agency, are entered in section 8.)

DEFENCE RESEARCH ESTABLISHMENT
DEPARTMENT OF NATIONAL DEFENCE
OTTAWA ONTARIO CANADA K1A 0K2

2. SECURITY CLASSIFICATION (overall security classification of the document, including special warning terms if applicable)

UNCLASSIFIED

3. TITLE (the complete document title as indicated on the title page. Its classification should be indicated by the appropriate abbreviation (S,C or U) in parentheses after the title.)

Chaotic Sea Clutter Returns
Current Status and Application to Airborne Radar Systems (U)

4. AUTHORS (Last name, first name, middle initial)

MC DONALD, MICHAEL K.

5. DATE OF PUBLICATION (month and year of publication of document)

NOV 2001

6a. NO. OF PAGES (total containing information. Include Annexes, Appendices, etc.)

66

6b. NO. OF REFS (total cited in document)

34

7. DESCRIPTIVE NOTES (the category of the document, e.g. technical report, technical note or memorandum. If appropriate, enter the type of report, e.g. interim, progress, summary, annual or final. Give the inclusive dates when a specific reporting period is covered.)

DREO TECHNICAL REPORT

8. SPONSORING ACTIVITY (the name of the department project office or laboratory sponsoring the research and development. Include the address.)

DEFENCE RESEARCH ESTABLISHMENT OTTAWA
DEPARTMENT OF NATIONAL DEFENCE
OTTAWA, ONTARIO, CANADA, K1A 0K2

9a. PROJECT OR GRANT NO. (if appropriate, the applicable research and development project or grant number under which the document was written. Please specify whether project or grant)

3DB29

9b. CONTRACT NO. (if appropriate, the applicable number under which the document was written)

10a. ORIGINATOR'S DOCUMENT NUMBER (the official document number by which the document is identified by the originating activity. This number must be unique to this document.)

DREO TR 2001-114

10b. OTHER DOCUMENT NOS. (Any other numbers which may be assigned this document either by the originator or by the sponsor)

11. DOCUMENT AVAILABILITY (any limitations on further dissemination of the document, other than those imposed by security classification)

(X) Unlimited distribution
( ) Distribution limited to defence departments and defence contractors; further distribution only as approved
( ) Distribution limited to defence departments and Canadian defence contractors; further distribution only as approved
( ) Distribution limited to government departments and agencies; further distribution only as approved
( ) Distribution limited to defence departments; further distribution only as approved
( ) Other (please specify):

12. DOCUMENT ANNOUNCEMENT (any limitation to the bibliographic announcement of this document. This will normally correspond to the Document Availability (11). However, where further distribution (beyond the audience specified in 11) is possible, a wider announcement audience may be selected.)

13. ABSTRACT (a brief and factual summary of the document. It may also appear elsewhere in the body of the document itself. It is highly desirable that the abstract of classified documents be unclassified. Each paragraph of the abstract shall begin with an indication of the security classification of the information in the paragraph (unless the document itself is unclassified) represented as (S), (C), or (U). It is not necessary to include here abstracts in both official languages unless the text is bilingual).

The potential to model sea clutter radar returns using chaos theory is examined. Chaotic systems display qualitative similarities to sea clutter returns such as broad flat spectrums, boundedness and irregular temporal behaviour. In this report several key parameters of chaotic systems, namely correlation dimension, Lyapunov spectrum and Lyapunov dimension are calculated from real sea clutter returns and found to be consistent with a chaotic interpretation. The airborne high resolution data (less than one metre) produces a correlation coefficient with an average value of 4.63 and an embedding dimension of 6-7. Lyapunov dimensions are consistent with correlation values. A local linear technique and a radial basis function (RBF) are used to construct a one step non-linear predictor. A Mean Square Error (MSE) of approximately 0.0032 between the predicted and normalized (i.e. maximum +/- 1 range) real time series is measured. If sea clutter is in fact, a chaotic system, then it may be possible to accurately predict sea clutter returns via a non-linear chaotic model and produce substantial improvements in the small target detection capabilities of the APS-506 radar on the CP-140 maritime patrol aircraft.

14. KEYWORDS, DESCRIPTORS or IDENTIFIERS (technically meaningful terms or short phrases that characterize a document and could be helpful in cataloguing the document. They should be selected so that no security classification is required. Identifiers such as equipment model designation, trade name, military project code name, geographic location may also be included. If possible keywords should be selected from a published thesaurus. e.g. Thesaurus of Engineering and Scientific Terms (TEST) and that thesaurus-identified. If it is not possible to select indexing terms which are Unclassified, the classification of each should be indicated as with the title.)

SEA CLUTTER
CHAOS
NON-LINEAR DETECTORS

Defence R&D Canada
is the national authority for providing
Science and Technology (S&T) leadership
in the advancement and maintenance
of Canada's defence capabilities.

R et D pour la défense Canada
est responsable, au niveau national, pour
les sciences et la technologie (S et T)
au service de l'avancement et du maintien des
capacités de défense du Canada.

DEFENCE R&D DÉFENSE

www.drdc-rddc.dnd.ca